5-4-2020

Dimer Pyruvate Kinase M2 Regulates de novo Collagen Synthesis and Crosslinking in Pathological Fibrosis

Ganesh Satyanarayana

DIMER PYRUVATE KINASE M2 REGULATES *de novo* COLLAGEN SYNTHESIS AND CROSSLINKING IN PATHOLOGICAL FIBROSIS

by

GANESH SATYANARAYANA

Under the Direction of Zhi-Ren Liu, PhD

ABSTRACT

Fibrosis is a pathologic condition of abnormal accumulation of collagen fibrils. Collagen is synthesized and secreted from myofibroblasts. Collagen is a major extracellular matrix (ECM) protein composed of mainly $(Gly\text{-}X\text{-}Y)_n$ triplets repeats with >30% Gly residue. During fibrosis progression, myofibroblasts must upregulate glycine metabolism to meet the need for collagen synthesis. We report here that pyruvate kinase M2 (PKM2) is upregulated in myofibroblasts. Myofibroblast differentiation promotes dimerization of PKM2. Dimer PKM2 slows the flow rate of glycolysis. Dimer PKM2 channels glycolytic intermediates to de novo glycine synthesis, which facilitates collagen synthesis and secretion in myofibroblasts. Our results show that PKM2 activator that convert PKM2 dimer to tetramer inhibits fibrosis progression in mouse models of liver and lung fibrosis. Furthermore, PKM2 activator alters glycolysis pathway, which

consequently affects the reverses fibrosis by reducing glycine production in vivo. Our study uncovers a novel role of PKM2 in tissue/organ, suggesting a possible strategy for treatment of fibrosis diseases. Furthermore, secreted collagen is crosslinked in the extracellular space by the lysyl oxidase (LOX) family proteins. LOX is secreted by the activated myofibroblasts under hypoxic conditions. PKM2 mediates Hif-1α activity in cells under hypoxic conditions. Here, we report that the PKM2- Hif-1α axis induces LOX expression in fibroblasts and cancer cells. PKM2-Hif-1α complex regulates LOX transcription by directly binding to LOX promoter. Here we show that PKM2 activators reduce PKM2-HIF1α association and thereby its nuclear localization. PKM2 activators reduce the production and hence the secretion and the crosslinking capacity of LOX family proteins.

INDEX WORDS: Pyruvate kinase M2, Fibrosis, Fibroblasts, Collagen, Metabolism, Serine, Glycine, Lysyl Oxidase, Hepatic Fibrosis, Pulmonary Fibrosis.

DIMER PYRUVATE KINASE M2 REGULATES *de novo* COLLAGEN SYNTHESIS AND CROSSLINKING IN PATHOLOGICAL FIBROSIS

by

GANESH SATYANARAYANA

A Dissertation Submitted in Partial Fulfillment of the Requirements for the Degree of

Doctor of Philosophy

in the College of Arts and Sciences

Georgia State University

2020

DIMER PYRUVATE KINASE M2 REGULATES *de novo* COLLAGEN SYNTHESIS AND CROSSLINKING IN PATHOLOGICAL FIBROSIS

by

GANESH SATYANARAYANA

Committee Chair: Zhi-Ren Liu

Committee: Ming Zou

Jing Chen

Ritu Aneja

Electronic Version Approved:

Office of Graduate Studies

College of Arts and Sciences

Georgia State University

May 2020

DEDICATION

I dedicate this dissertation to my family, who gave me great spiritual and financial support selflessly for my pursuit of knowledge for the past five years. To all my teachers who have been a part of my learning process through my childhood. To all my friends who have supported me through the years.

ACKNOWLEDGEMENTS

I may be the purveyor of this dissertation but there are many people behind the scenes who have been a source of great inspiration and support in making my journey successful.

I offer my gratitude to the plethora of people who were present to support me during my doctoral pursuit. My primary thanks go to my advisor, Dr. Zhi-Ren Liu, who has provided me an opportunity to join his lab back when I was a fresh off the block undergraduate with very little research experience. He took me in and has supported me through failed hypotheses and has guided me onto the right path. I thank him for the immense trust he put in my hypothesis and allowed me to pursue my work independently and voice my opinions. The members of my committee, Dr. Aneja and Dr. Ming Zou, have always been ready with suggestions when I needed guidance.

This dissertation would have been impossible without the support of my fellow graduate students from various laboratories who have helped me in a spectrum of issues from laboratory-based experiments to support in my personal life. I extend my thanks to Dr. Liangwei Li, Dr. Yinwei Zhang, Chakravarthy Garlapati, Neha Panchbhai, Heena Sadhwani, Malvika Sharma, Falguni Mishra, Guangda Peng, Hongwei Han and Yang Huang who have helped me in various ways without which I wouldn't have completed my doctoral studies.

I would like to thank the staff of the biology department, LaTesha Warren, Tameka Hudson, Larialmy Allen, Sonja Young, Debbie Walthall, Mary Karom, who were quick to resolve any issues that I have faced as a graduate student in these years. I would also like to thank the staff of DAR, Dr. Michael Hart, Courtnye Billingsley, Joi Scott, Michael Morrison and Matthew Davis who have helped me in the handling and designing experiments with mice. I would also like to thank Dr. Francisco Cruz and Julie Stowell, who have given me an opportunity to learn the art of teaching by graciously offering me a TA position for many semesters.

Special thanks go to Dr. Ravi Chakra Turaga, a postdoctoral scholar in my lab and a close friend. He has taken me under his wing when I first entered the program and has trained and molded me into the researcher that I am today. My doctoral journey would have been moot if not for his guidance and his suggestions in experimental design. He was always present to spitball ideas and have scientific debates. I thank him for his maturity and his efforts into guiding me in both my personal and professional endeavors.

I thank Radhakishen Jayanti, Aishwarya Chitta, Bharat Nowduri, and Sandeep Kandukuri who have been in my life for more than a decade, without whom I would have not had the mental strength to finish my PhD. I would like to thank Rajesh Venkatesh for always keeping me company through my late-night study sessions and putting things into perspective when I was burdened.

My thanks would not be complete without thanking Shreya Thacker. She was my emotional support system through my PhD, and she has always put my needs first and selflessly helped me in all these years. I am completely indebted to her for all the times she has fed me when I had no energy to cook and took care of the house when I had no energy to clean. She deserves this award as much as I do for putting up with me for all these years.

Lastly, I would not be in this position without the tremendous support of my family, Satyanararayana Pamidipati, Padma Pamidipati, Reethika Pamidipati who have always supported my career choices and have forgiven me for my mistakes and always pushed me towards excellence at every walk of life.

There are a lot of people who I might have missed in this list, and to all of you, please know that you will always be remembered for your help and support.

TABLE OF CONTENTS

LIST OF TABLES

LIST OF FIGURES

LIST OF ABBREVIATIONS

BSA	Bovine serum albumin
cDNA	complementary DNA
DNA	Deoxyribonucleic acid
DTT	Dithiothreitol
EDTA	Ethylenediaminetetraacetic acid
FPLC	Fast performance liquid chromatography
HRP	Horse radish Peroxidase
MTT	3-(4,5-Dimethylthiazol-2-yl)-2,5-diphenyltetrazolium bromide
mg	Milligram
µg	Microgram
mL	Milliliter
mM	10^{-3} mol/dm^3
µM	10^{-6} mol/dm^3
MW	Molecular weight
ng	Nanogram
nm	nanometer
nM	10^{-9} mol/dm^3
O. D.	Optical Density (Absorbance)

PBS	Phosphate buffer saline
PCR	Polymerase chain reactions
pM	10−12 mol/dm3
SDS-PAGE	Sodium dodecyl sulfate polyarcylamide gel electrophoresis
Tris	2-Amino-2-(hydroxymethyl)-1,3-propanediol
UV	Ultraviolet
APC	Antigen presenting cell
CTLs	Cytotoxic T lymphocytes
EC	Endothelial cell
E. coli.	Escherichia coli
ECM	Extracellular matrix
EGF	Epidermal growth factor
FBS	Fetal bovine serum
FGF	Fibroblast growth factor
FGFR	Fibroblast growth factor receptor
EPC	Endothelial progenitor cell
FIGF	Fos-induced growth factor
FLK	Fms-like tyrosine kinase
HCC	Hepatocellular carcinoma
HIF	Hypoxia-inducible factor
IF	Immunofluorescence

IgSF	Immunoglobulin superfamily
INF	Interferon
IL	Interleukin
i.p.	Intraperitoneal
mAb	Monoclonal antibody
mTOR	Mammalian target of rapamycin
NK cell	Natural killer cell
PCR	Polymerase chain reaction
TGF	Transforming growth factor
G6P	Glucose-6-Phosphate
F6P	Fructose-6-Phosphate
F-1,6-BP	Fructose-1,6-bis Phosphate
G3P	Glyceraldehyde-3-Phosphate
1,3-BPG	1,3-Bisphosphoglycerate
3PG	3-Phosphoglycerate
2PG	2-Phosphoglycerate
PEP	Phosphoenolpyruvate
DAP	Dihydroxyaccetonephosphate
PFK	Phosphofructokinase
PFI	Phosphofructoisomerase
PKM1	Pyruvate Kinase M1

PKM2	Pyruvate Kinase M2
PDH	Pyruvate dehydrogenase
PHGDH	Phosphoglycerate dehydrogenase
ATP	Adenosine-triphosphate
ADP	Adenosine-diphosphate
AcCoA	Acetyl Co-enzyme A
TCA	Tricarboxylic acid
SAR	Structure activity relationship
	Miscellaneous
ATCC	American type Culture Collection
DAR	Department of Animal Research
GSU	Georgia State University
IACUC	Institutional Animal Care and Use Committee
Rpm	Revolutions per minute

1 INTRODUCTION

1.1 GLYCOLYSIS

1.1.1 Physiological Glycolysis

Glycolysis is an energy conversion pathway is many organisms. This pathway exists commonly in all organisms, both prokaryotic and eukaryotic cells. In eukaryotic cells, glucose enters through the GLUT family of receptors. Glucose is then metabolized by a series of enzymatic reactions in the cytosol. These enzymatic reactions are broadly classified into three stages. Stage 1 is a phosphorylation event which traps the glucose in the cell. In the first phosphorylation event, glucose is converted into G6P by hexokinase. G6P is then converted into F6P by PFI and then a second phosphorylation step leads to the formation of F-1,6-BP. Stage 2 comprises of cleavage events where the 6-carbon glucose/fructose units are cleaved into 3 carbon units. The reaction then proceeds to stage 3. Herein, the 3 carbon units are interconvertible, and ATP is synthesized when they are oxidized to pyruvate in the final step of glycolysis. Pyruvate is then readily oxidized into AcCoA in the mitochondria which then enters the citric acid cycle or the tricarboxylic acid cycle to produce ATP via oxidative phosphorylation (figure 1.1) (Berg, Tymoczko et al. 2015).

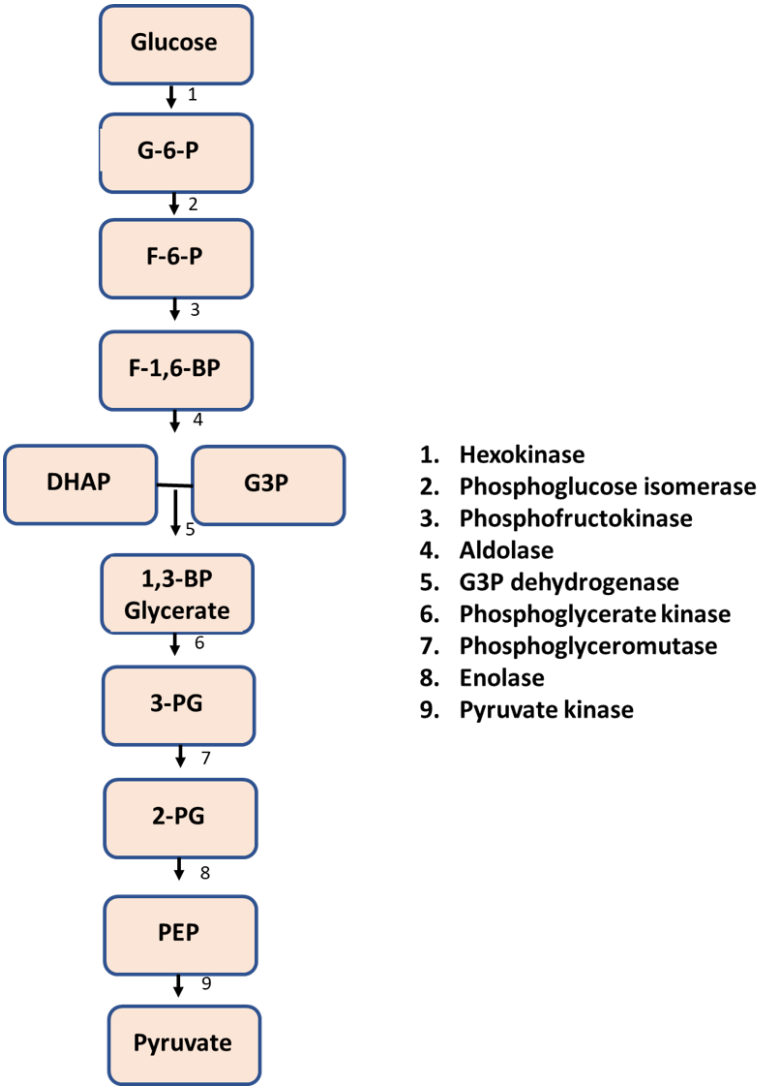

Figure 1.1 Glycolysis – An overview.

This figure illustrates the flow of glucose through the various stages of glycolysis, undergoing several phosphorylation and oxidation events to produce pyruvate and ATP.

Energy requirements in the cell are primarily met by the conversion of glucose into pyruvate which yields 2 molecules of ATP per glucose molecule. Pyruvate is oxidized by PDH into AcCoA in the mitochondria. The generated AcCoA enters the TCA cycle by reacting with

oxaloacetate to form citrate. Citrate is then moved through several enzymatic reactions to yield oxaloacetate again which feeds into the TCA cycle forming a closed metabolic loop. The total yield of ATP from the TCA cycle is 2 per molecule of pyruvate which enters the mitochondria. While the TCA cycle itself yields only 2 ATP molecules, these are from substrate level phosphorylation. Most of the ATP yield comes from the generation of high energy molecules, NADH and $FADH_2$ which participate in the electron transport chain to yield 15 and 3 ATP molecules per molecule of glucose respectively. Therefore, the total net gain of ATP from one molecule of glucose is around 30-32 molecules of ATP (figure 1.2) (Ryan, Murphy et al. 2019).

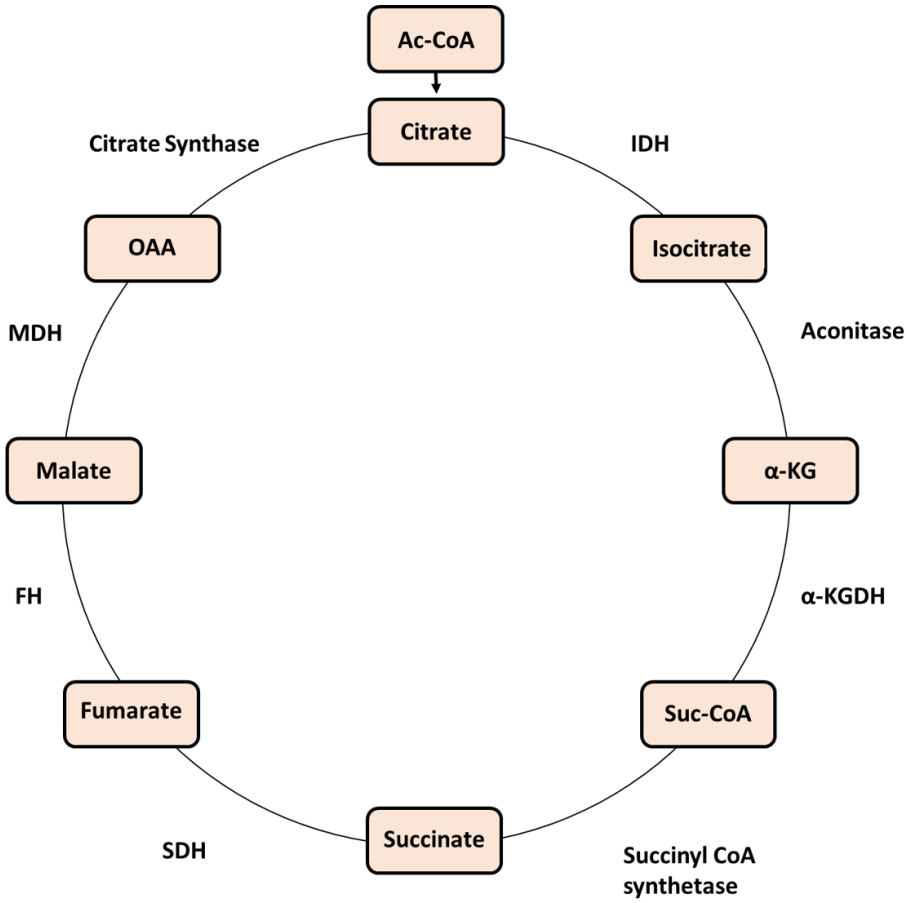

Figure 1.2 TCA cycle.

This figure depicts the movement of pyruvate through the energy generating steps of the TCA cycle in the mitochondria, thus generating high energy NADH and $FADH_2$ which feed into the electron transport chain.

1.1.2 Warburg Effect

Glycolysis in proliferating cells is altered to suit their metabolic needs. Proliferating cells need more ATP in order to meet their biosynthetic requirement. Along with the increased ATP need, the dividing cells incur a large requirement of nucleotides, amino acids, and lipids. To meet with this increased requirement, these cells switch to an altered metabolic state known as the Warburg effect. During the advent of Warburg effect, these cells switch away from oxidative phosphorylation by redirecting the pyruvate to lactate instead of transporting into the mitochondria. By doing so, these cells switch to a less efficient way to produce ATP. During physiologic glycolysis, one molecule of glucose yields anywhere between 30 to 36 molecules of ATP. But, during the Warburg phase, these cells yield only around 4 moles of ATP per glucose molecule.

Given the lower amounts of ATP produced per molecule of glucose, how do these proliferating cells remain viable is a big question. During division, ATP hydrolysis usually provides energy for many of the biochemical reactions responsible for replication. Apart from these reactions, these cells have other requirements which extend beyond ATP. These requirements generally include amino acids, nucleotides and fatty acids. In dividing cells, the most consumed nutrients are glucose and glutamine, therefore, these molecules are the main source of ATP. But directing all these nutrients solely towards oxidative phosphorylation to maximize ATP output is counterintuitive to proliferating cells. These cells need other macromolecules in order to divide, and the Warburg effect shunts the carbons from glucose into production of AcCOA for

fatty acid synthesis, glycolytic intermediates for amino acid synthesis and the pentose phosphate pathway for NADPH and nucleotide synthesis. Therefore, all proliferating cells adopt this altered form of glycolysis to reduce ATP output and shunt glycolytic intermediates towards anabolic process of the biomacromolecules required for cell division (figure 1.3) (Vander Heiden et al., 2009).

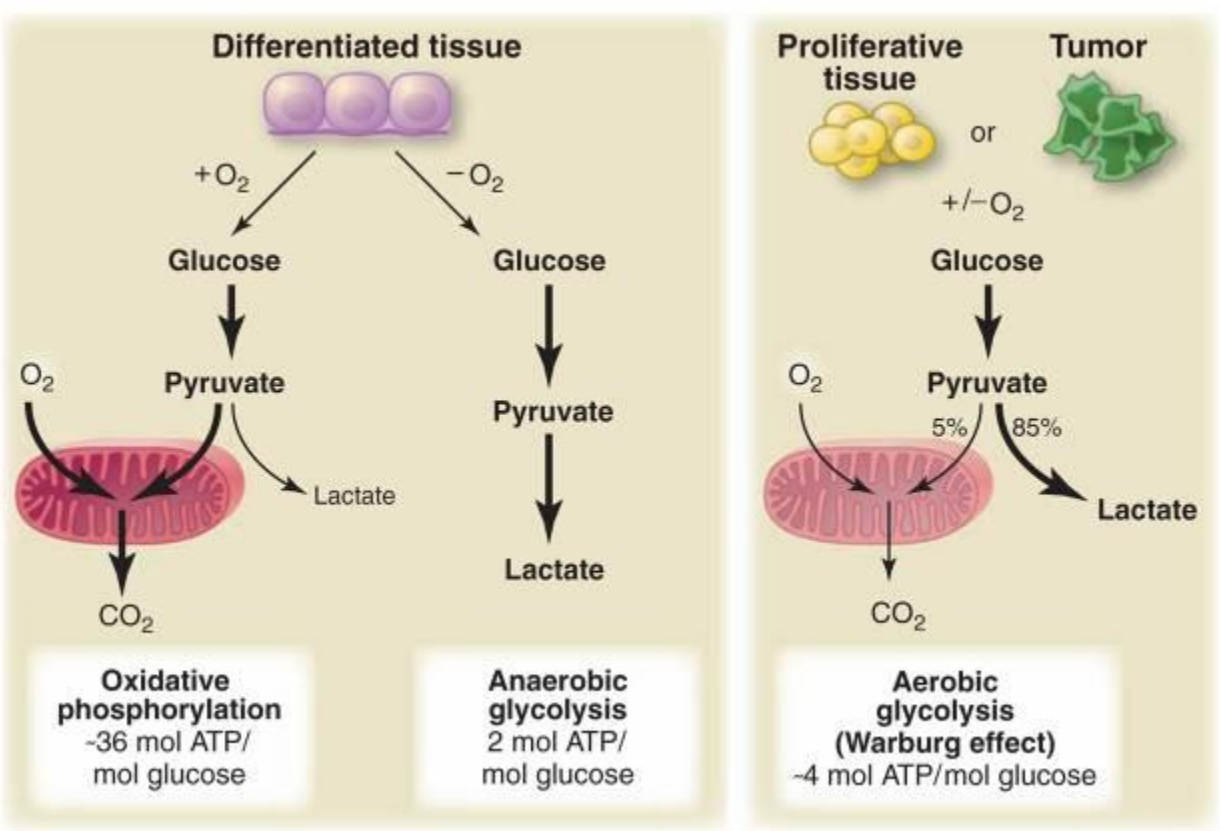

Figure 1.3 The Warburg effect

This figure demonstrates the altered states of glycolysis undertaken by cells based on their proliferative state and metabolic demand.

1.2 PYRUVATE KINASE

1.2.1 Alternative splicing of M gene

Pyruvate kinase (PK) is the final rate limiting step in glycolysis. PK catalyzes the phosphorylation of ADP into ATP from PEP. PK has 4 isoforms PKM1, PKM2, PK-L and PK-R. These isoforms have differential expression in different tissues. PK-L and PK-R are expressed in the liver and erythrocytes respectively. PKM1 and PKM2 are expressed in various tissues. PKM1 is found in all adult tissues and PKM2 is found in embryonic tissues. PKM2 is also found in several tumor types and is widely implicated in altered metabolic states in tumors.

The PKM gene is alternatively spliced to form transcripts which are encoded to either PKM1 or PKM2. Both M1 and M2 transcripts have 12 exons and the inclusion of either exon 9 or exon 10 dictates the generation of PKM1 and PKM2 respectively. The generation of these isoforms requires the inclusion of exon 9 to generate PKM1 and to generate PKM2, exon 9 is repressed and exon 10 is included. Exon 9 repression and subsequent exon 10 inclusion is tightly controlled by the heterogeneous nuclear ribonucleoprotein (hnRNP) family of proteins. hnRNPA1 and hnRNPA2 aide in the repression of exon 9 therefore leading to the inclusion of exon 10. Exon 10 inclusion also requires the binding of the serine/arginine-rich splicing factor 3 (SRSF3) protein to exon 10. The alternative splicing of the M gene is tightly controlled by multiple repressors and the SRSF3 mediated inclusion. These factors contribute to the expression of PKM2.

1.2.2 PKM in glycolysis

Pyruvate kinase catalyzes the final step of glycolysis. Herein, the high energy phosphate group from phosphoenolpyruvate (PEP) is transferred to adenosine diphosphate (ADP) and yields adenosine triphosphate (ATP) and pyruvate. Catalysis occurs by simultaneous binding of PEP and ADP to the active site of pyruvate kinase by complexing with Mg^{2+} cation. The

phosphate group from PEP is transferred to ADP leaving the less stable enol form of pyruvate bound to pyruvate kinase. The enolpyruvate is then tautomerized by accepting a proton from a water molecule. The products then leave the active site following tautomerization. Both PKM1 and PKM2 share primary and tertiary structures for the active sites and therefore exhibit similar substrate binding specificities. Apart from ADP, pyruvate kinase can also catalyze the transfer of phosphate group to guanine diphosphate (GDP), uridine diphosphate (UDP) and cytidine diphosphate (CDP). Though these substrates can be phosphorylated by pyruvate kinase, their binding affinity is lower than that of ADP.

Pyruvate kinase is a tetrameric protein of identical monomers. Each monomer is comprised of A, B and C domains and a small N-terminal domain. The A domain is the largest domain containing a symmetrical triosephosphateisomerase (TIM) barrel arrangement of 8 alpha-helices and 8 parallel beta sheets. The active site of the enzyme is located at the end of the α_8/β_8 TIM barrel. The B domain is a mobile domain which closes the active site upon binding to the substrate-Mg^{2+} ion complex. The C domain is present on the opposite side of the A domain and contains the binding site for fructose 1,6 bisphosphate (FBP). This domain placement is common to all isoforms of PK except for domain C which is different in PKM2 isoform which is encoded by exon 10 inclusion.

The tetramer is arranged in a dimer of dimers configuration, wherein a homodimer is bound to another homodimer. The dimer-dimer interaction is via the C domains of the two subunits. The amino acids encoded in the C domain is different in the M1 and M2 isoforms and are responsible for the differences in binding of FBP and subsequently its allosteric regulatory functions. The tetramer conformation of PK is the most active form. PKM1 is a constitutively active tetramer but also retain catalytic activity in its dimer form. Unlike PKM1, PKM2 is not a constitutively active

tetramer. PKM2 isoform can undergo reversible association and disassociation of the active tetramer conformation under certain conditions. Dilution of PKM2 leads to the disassociation of the active tetramer into its dimer form and thus loses its catalytic activity. In this condition, the activity of PKM2 is only at 4% of that of the tetramer. This reversible activation of PKM2 by FBP allows for regulation of its enzymatic activity.

1.2.3 Activators and Inhibitors of PKM2

The interchangeable conformations of PKM2 allows it to be activated and inhibited by various factors thus leading it to be in dimer or in tetramer states. Tetramer PKM2 is the most active isoform and has the most glycolytic activity. The activation of PKM2 is commonly potentiated by FBP in a physiological system. In the absence of these activators, PKM2 has a low affinity to PEP and the affinity of PEP is increased in the presence of glycolytic intermediate, fructose-1,6-bisphosphate.

FBP binds to PKM2 at a distinct site away from the active site and upon binding, increases PEP affinity and promotes tetramerization. This FBP-bound PKM2 is now in its active state leading to increased glycolysis. FBP is an allosteric activator only for PKM2 but not PKM1 due to structural differences at the binding pocket. PKM1 exists as a stable tetramer that has constitutive activity and does not require allosteric activation. PKM1 and FBP-bound PKM2 are identical in their kinetic parameters. They both exhibit the same three-dimensional conformation with the structural differences only in the areas encoded by the differential exons 9-10. PKM1 and PKM2 differ only in their FBP binding site and its dimer-dimer interface.

Apart from FBP, there are several other activators which can bind to PKM2 and allosterically activate it. Most of the activators are amino acids and other non-glycolytic metabolites, which allows for regulation of PKM2 activity with other metabolic pathways in the cell. Although these metabolites bind to PKM2 and allosterically activate it, they usually require high concentration. Phenylalanine (Phe) and alanine (Ala) are some of the few amino acids which can bind to PKM2. Phe and Ala are both allosteric inhibitors of PKM2.

Phenylalanine reduces both PKM1 and PKM2 activity by decreasing its affinity to PEP. The Phenylalanine binding site is distinctly different from the FBP binding site and the active site.

Phe-bound PKM2 stays in a unique conformation state wherein the active site is left in an open conformation and stabilizes PKM2 in its tetramer state but in an inactive state. This inactive state of PKM2 can only be partially reversed by FBP binding. Alanine on the other hand has a different mechanism of allosteric inhibition. When alanine is bound to PKM2, it favors the formation of the dimer state. However, the binding of alanine is completely reversed by the binding of FBP thus stabilizing the tetramer state. Serine is an allosteric activator of PKM2, and it is a direct competitor of alanine and binds to the same binding pocket.

A non-amino acid inhibitor of PKM2 is the thyroid hormone T3. Triiodo-L-thyronine (T3) is an allosteric inhibitor of PKM2. T3 binds to the monomeric form and stabilizes it in its inactive monomeric state. Allosteric inhibition of PKM2 by T3 can be reversed in the presence of FBP. An intermediate of *de novo* purine synthesis pathway is succinylaminoimidazolecarboxamide ribose-5-phosphate (SAICAR) is an allosteric activator of PKM2. However, it does not bind to any other M isoforms. PKM2 activity can also be modulated by synthetic activators. These designed molecules bind to the dimer-dimer interphase of PKM2 and sequesters PKM2 in its active tetrameric state. These molecules can bind to the dimer form of PKM2 in nanomolar concentrations. The binding site of the synthetic activators is distinctly different from the FBP binding site and whether the synthetic molecule binding site can be occupied by endogenous activators is currently unknown.

1.2.4 Synthetic Activators

Activators of PKM2 have been synthesized by two different classes of compounds, the diarylsulfonamides and the pyridazinones. The diarylsulfonamide class of activators are substituted in their R-groups and are classified as the *N, N'*-diarylsulfonamides analogues. These analogues are synthesized by a series of coupling, deprotection and a second coupling reaction.

Mono-boc protected piperazine is coupled to aryl sulfonyl chloride to yield boc-protected *N*-arylsulfonamides. The intermediates are then deprotected and subsequently coupled to another substituted *N*-arylsulfonamide to yield *N, N'*-diarylsulfonamides. The ***d***i***a***ryl***s***ulfon***a***mide class compounds are designated as DASA. In the numerous compounds tested, DASA-10 and DASA-58 are the most efficient in increasing the activity of PKM2. The pyridazinone class of activators are substituted ***t***hi***e***no[3,2-b]***p***yrrole[3,2-d]***p***yridazines. These class of compounds require a series of reaction schemes (Jiang et al., 2011). The pyridazinone class compounds are designated TEPP. Of the numerous TEPP family compounds tested, TEPP-46 are the most efficient in increasing the activity of PKM2.

All the above-mentioned synthetic activators, in both classes, DASA-10, DASA-58 and TEPP-46, are selective only for PKM2 and have no binding efficiency towards PKM1. This is consistent with the lack of allosteric regulation in PKM1. Crystallography studies with the activators show that one active tetramer contains 2 molecules of the activators and 4 molecules of FBP which indicates that the activators bind to different sites than that of FBP. FBP binds to the C-C interface between the two dimers of PKM2. The activators bind deep within the A-A interface of the dimer pair. The activator binding pocket accommodates the molecules via polar interactions and van der Waals forces with the pocket lining residues.

Once bound to the dimer-dimer interface, these activators force the tetramer conformation of PKM2 and increase its binding affinity to PEP therefore increasing the glycolytic activity of PKM2. The selective synthetic activation of PKM2 promotes the resolution of Warburg effect usually observed in proliferating cells, most widely observed in cancer cells. Due to this, there are many metabolic changes that occur within the cancer cells when treated with PKM2 activators. These metabolic changes mimic that of the cells which express PKM1. When treated with the

activators, the PK activity is increased by around 60% thereby depleting the glycolytic intermediates formed in the advent of Warburg effect in these cells. Since the PK activity is increased, the shunting of pyruvate into lactate is reduced and the increased pyruvate is shunted into tricarboxylic acid (TCA) cycle. Glycolytic intermediates can be used for the *de novo* lipid synthesis and treatment with PKM2 activators reduce lipid production from glucose. They also reduce the lipogenic acetyl-CoA produced from glucose. Almost all the anabolic pathways branching from glycolytic intermediates are thereby reduced upon treatment with activators. The anabolic pathways include NADPH production from the pentose phosphate pathway, serine from *de novo* amino acid synthesis, ribose-5-phosphate from *de novo* purine synthesis pathway. The properties of these activators are tested in a variety of cancers and they show similar affinity to PKM2 *in vitro* as well as *in vivo*.

1.2.5 Regulation of PKM2

Pyruvate kinase can be phosphorylated in the cell in response to extracellular signaling. These signaling events are usually in response to a growth factor mediated tyrosine phosphorylations. Upon growth factor action, several intracellular kinases are activated and can phosphorylate a myriad of proteins. PKM2 can be readily phosphorylated at the Y105 residue by c-Src kinase. Upon phosphorylation, PKM2 is inactivated thus reducing its kinase activity. PKM2 has a phosphor-tyrosine binding binding domain upon binding to which releases bound FBP from its binding pocket. This release of FBP renders PKM2 inactive in its dimeric form thereby reducing its activity.

Phosphor-tyrosine binding nature of PKM2 makes up for its relative abundance in a cancer cell. Since tyrosine phosphorylated proteins can bind to multiple tetramers of PKM2 and release bound FBP, it allows for reduction in PKM2 activity despite a low tyrosine phosphorylated protein

to PKM2 ratio in the cell. The interaction between PKM2 and phosphor-tyrosine residues is dependent on the K433 residue on PKM2. Tyrosine phosphorylation yields a net negative charge to which the positively charged side chain of K433 can bind. The relevance of this interaction is due to the presence of the FBP binding site present at this location. The lysine side chain directly interacts with the phosphate group on FBP. Therefore, the binding of phosphor-tyrosine can directly interact with the PKM2-FBP binding and promote its release from the binding pocket thus reducing its activity.

PKM2 is phosphorylated on its tyrosine residue Y105. Phosphor-PKM2 can now act as a binding partner to the K433 residue and facilitating the release of FBP from the tetramer binding pocket. The interaction between Y105 phosphorylated PKM2 and an FBP-bound PKM2 leading to FBP release leads to the inactivation of PKM2 and sequesters it in its dimer form. FBP has an AC50 value of around 7μM, so the ability of FBP to be bound to PKM2 and restrain it in its active tetramer is very high as the intracellular concentration of FBP is around 80μM. The reversal of the ability of FBP to be bound to the highly expressed PKM2 under intracellular concentrations of FBP requires consistent growth factor stimulation and subsequent tyrosine phosphorylation of downstream proteins, including PKM2 itself. This sustained growth factor signaling and phosphor-tyrosine binding of PKM2 and its continual release of FBP keeps PKM2 is a continuous state of inactivity. This growth factor fueled inactivity of PKM2 signifies the relationship between glycolysis and tyrosine signaling and the subsequent buildup of glycolytic intermediates.

1.2.6 Non-canonical functions of PKM2

The canonical function of PKM2 is the glycolytic phosphorylation of ADP using PEP as the donor of its high energy phosphate group. This reaction occurs by simultaneous binding of PEP and ADP to their respective binding sites. Binding of ADP to the active site can double as a

binding site for other proteins wherein upon binding they get phosphorylated using PEP as the phosphate source. Therefore, PKM2 can act as a protein kinase with albeit using PEP instead of ATP. Tetrameric PKM2 in its FBP bound state can innately bind to ADP in its active site and phosphorylate it thus carrying out its glycolytic function leading to the production of pyruvate whereas dimeric PKM2 facilitated by the release of FBP from its binding site is rendered inactive either by its phosphorylation, acetylation or succinylation.

In the cytoplasm, PKM2 can bind to HuR, an RNA binding protein which plays a role in mRNA stability and translational efficiency. PKM2 is found to be a binding partner of tristetraprolin, an mRNA binding protein. After binding to tristetraprolin, it phosphorylates it and leads to is degradation and upregulates breast cancer proliferation. The mitochondrial anti-protein Bcl2 is a binding partner of PKM2. Under oxidative stress, PKM2 translocates to the mitochondria wherein PKM2 phosphorylates Bcl2 at T69 and is stabilized. Phosphorylated Bcl2 does not undergo ubiquitination, therefore PKM2 aids in the adaptation of cancer cells to oxidative stress.

Dimeric PKM2 can relocate to the nucleus under specific stimuli. In the nucleus, dimer PKM2 has a multitude of functions. It serves in the regulation of transcription and epigenetic modifications. Upon EGFR activation, β-catenin is phosphorylated at Y333. Phosphor-β-catenin can now bind to PKM2 and this complex is translocated to the nucleus. In the nucleus, this complex binds to the CCND1 promoter and leads to HDAC3 removal, histone acetylation and cyclin D1 transcription. It can also phosphorylate stat3 at Y705 leading to its binding to MEK5 promoter and upregulates cell proliferation. Beside transcription factor activation, PKM2 has been shown to phosphorylate MLC2, BUB3 and ERK1 and ERK2. It can also associate with NF-κB and HIF-1α to promote angiogenesis by activating the expression of the HIF response element (HRE) target gene VEGF-A. Upon binding to HIF-1α in bone marrow derived macrophages (BMDM), PKM2-

HIF-1α complex upregulates the transcription of IL-1β and upregulate a pro-inflammatory response in these macrophages. With the increasing evidence of the nuclear relocation and function of PKM2, there is some evidence to support the contrary. Using [^{32}P]-labeled PEP and PKM2 null mice experiments, some evidence exists that PEP dependent phosphorylation is not a common occurrence in cells.

Extracellular PKM2 is a recently researched area wherein PKM2 is packaged in exosomes and secreted out of the cell and into the extracellular space. PKM2 is a packaged protein in these exosomes and has a communicative role between host and recipient cells. Secreted PKM2 is shown to have angiogenic properties, wherein, PKM2 promotes tumor growth by increasing the proliferation, migration and tube formation properties of endothelial cells. PKM2 secreted by colon cancer cells acts via autocrine signaling and activates cell migration via the PI3K/AKT and the WNT/β-catenin pathway. Apart from cancer cells, PKM2 secretion has been observed to be secreted from neutrophils and aids in wound healing via activation of endothelial cells and promotes angiogenesis. PKM2 is also shown to bind to EGFR and phosphorylate it and activates EGFR pathway leading to cell proliferation in breast cancer cells. Liquid chromatography/mass spectrometry (LC/MS) analyses show that the secreted PKM2 is the dimer form of PKM2. Mutant PKM2 (R399E) is mostly in its dimer form and dimer PKM2 has better extracellular response than its tetrameric form.

1.3 COLLAGEN

1.3.1 Collagen in Physiology

Collagen is the most abundant protein in vertebrates. Collagen consists of a right-handed bundle of three parallel, left-handed polyproline type-2 helices. There are several types of collagen and are classified based on their distribution, composition and pathology. The categories

are fibrillar, network forming, fibril-associated collagens with interrupted triple helices (FACIT), membrane-associated collagens with interrupted triple helices (MACIT) and multiple triple helix domains and interruptions (MULTIPLEXIN). Twenty-eight different collagens have been identified and they are of different categories mentioned above.

The structural motif of collagen has three parallel polypeptide strands in a left-handed polyproline type 2 helical coil. This helical coil is a tightly packed triple helix which mandates glycine to be every third residue in the peptide strand. The resulting repeating sequence is denoted as XaaYaaGly sequence. The Xaa and Yaa could be any other amino acid. The Xaa and Yaa are often proline and hydroxyproline respectively. The ProHypGly conformation is the most common triplet found in collagen. These triple helices are known as tropocollagen (TC), assemble to form macroscopic fibers which is found in tissue, bone and basement membranes. All members of the collagen family are secreted proteins and are deposited as the part of the extracellular matrix (ECM). All the collagens in the ECM is arranged in supramolecular assemblies. The collagens in the ECM play a mechanical role in the structural organization of the tissue.

Fibrillar collagens are the principal source of tensile strength in animal tissues. They are of indeterminate length and vary in their diameter from 12nm to >500nm. The fibrils are in a periodic structure and it is due to regular staggering of triple helical assembly. The XaaYaaGly organization of collagen is a part of fibrillar collagen and contains about 1000 residues and is an uninterrupted chain. Fibrillar collagens are synthesized as pro-collagens with the N and C propeptides at the end of each triple helical domains. The propeptides are cleaved by pro-collagen N or C proteinases. The pro-collagen N-proteinase belongs to the A Disintegrin And Metalloproteinase and Thrombospondin motifs (ADAMTS) family. The pro-collagen C-proteinase belongs to the Bone Morphogenic Protein (BMP) family. Cleavage of pro-collagens by these proteinases exposes the

telopeptide sequences which are short non-triple helical extensions of the chains. The fibrils are stabilized a non-reducible covalent crosslink between the triple helix and the telopeptides. These crosslinked peptides are essential for the mechanical maintenance of tissues.

Individual proα chains undergo numerous post translational modifications which include hydroxylation of proline and lysine residues, glycosylation of lysine and hydroxyproline residues, sulfation of lysine residues. Once these modifications are completed, the assembly of the triple helix chain commences, and the formation of the triple helix ceases any further post translational modifications. In the endoplasmic reticulum, procollagen is bound to its chaperone protein, heat shock protein 47 (HSP47). The binding of HSP47 to the triple helix is required for its stabilization. Another protein, secreted protein acidic and rich in cysteine (SPARC), might also act as a chaperone for collagen, as its absence leads to defective collagen deposition and mechanical organization of tissues.

1.3.2 Collagen in Fibrosis

During the advent of fibrosis, activated fibroblasts are triggered by fibrotic stimuli which include the pro-inflammatory response from the infiltrated macrophages. The major cytokine released by these pro-inflammatory macrophages is transforming growth factor – beta (TGF-β). TGF- β is the major activator of quiescent fibroblasts residing in the organ. These fibroblasts are activated by TGF- β binding to two of its receptors TGF□R1-R2 dimers to form a heterotetrameric receptor complex. The receptor is then auto-phosphorylated to trigger downstream signaling through secondary messengers. Canonical signaling of TGF- β is usually triggered by the phosphorylation of SMAD family of proteins at their SSXS (Ser-Ser-X-Ser) motif. This activation triggers the formation of a complex consisting of 2 rSMADs and one common SMAD (SMAD4). This complex then localizes to the nucleus and triggers gene transcription. The rSMADs binding

to the co-SMAD, SMAD4 regulate the genes transcribed by the upstream signal. During the activation event of fibroblasts by TGF- β triggers the phosphorylation and activation of SMAD3 which was figured to be the major SMAD responsible for the activation of fibroblasts. The involvement of other SMADs is relatively non-implicative in the activation of fibroblasts (Gu et al., 2007).

The trigger of SMAD3 activation in fibroblasts triggers the transcription for an array of genes which mark the activation of fibroblasts. The upregulation of alpha-smooth muscle actin converts the fibroblasts into mechanically tensile cells capable of contractile function. These special cells are termed as myofibroblasts. The activated myofibroblasts have a plethora of genes that are activated along with αSMA and one such gene is COL1A1. COL1A1 is the principle gene responsible for the transcription of collagen-1, which is one of the major fibrillar collagens. Collagen-1 is typically known to be a response towards a wound and it facilitates wound healing and repair. Under consistent activation of these fibroblasts, the synthesis and secretion of collagen-1 is not restricted and leads to increased accumulation of collagen-1 in the extra cellular matrix (ECM). The deposition of collagen-1 in the ECM is a key factor in the initial trigger of tissue hardening and the onset of fibrosis.

In pathological fibrotic conditions, the activation signal for the differentiation of fibroblasts is consistent due to the continuous pro-inflammatory signaling present in the tissue parenchyma. Moreover, the secreted collagen from previously activated myofibroblasts can act as an activation trigger for quiescent fibroblasts thus activating them to synthesize and secrete more collagen into the extracellular matrix. This pathological positive feedback loop of collagen synthesis, its secretion and the further activation of quiescent fibroblasts is a major hallmark of fibrosis. The secreted collagen-1 exhibits fully crosslinked form which is resistant to the action of matrix

mettaloproteinases (MMPs) thereby do not resolve with the attenuation of the fibrotic insult. The MMPs are usually secreted by the myofibroblasts during the initial wound healing phase to actively degrade the secreted collagen to prevent its pathological accumulation in the ECM. Upon continued stimulus, however, these fibroblasts secrete several lysine deaminase and lysine oxidase family of lysine crosslinking enzymes which promote the pathological accumulation of collagen in these fibrotic organs leading to their subsequent failure (Hernandez-Gea et al., 2011).

1.3.3 Modifications of secreted collagen

Collagen is a complex secreted protein consisting of three separate alpha helical strands which assemble into trimers and are then modified in the endoplasmic reticulum via several post translational modifications and then are secreted out of the cell. These modifications include the hydroxylation of two residues lysine and proline. Proline is the second most abundant amino acid in collagen after glycine and lysine is also found in high quantities in the collagen alpha strands. The modification of these residues is therefore relatively simple and happens frequently. The modification of these residues confers increased stability between the alpha strands of the collagen trimer.

The modifications that occur in the endoplasmic reticulum is the hydroxylation of proline and lysine wherein, the hydroxylation of proline is the most abundant protein post-translational modification in humans. This modification is catalyzed prolyl-4-hydroxylase (P4H) and its action yields the production of (2*S*, 4*R*)-4-hydroxyproline (Hyp). The hydroxylated residue is usually present in the Xaa-Yaa-Gly repeat right after the proline residue in the Yaa position. Hydroxyproline stabilizes the triple helix structure of collagen by a stereoelectronic effect and increases the thermal stability of collagen by lowering its T_m by 15C. The catalysis of Hyp is crucial for the folding and formation of the secondary triple helix and is dependent on the presence

of alpha-ketoglutarate (αKG) and ascorbic acid. P4H is a non-heme iron(II) αKG dependent dioxygenase family enzyme wherein αKG is decarboxylated and oxidized to form succinate. Ascorbic acid is a co-factor in the production of Hyp. During P4H activity, it can catalyze the decarboxylation of αKG without effecting the hydroxylation of proline which leads to the decoupling of the reaction. Ascorbic acid rescues this decoupling by reducing the inactive iron (III) to active iron (II) thereby aiding in the effective hydroxylation of proline. Deficiency in ascorbic acid leads to unstable collagen fibers causing scurvy. Therefore, this single post translational modification of collagen regulates the pathological synthesis and secretion of collagen (Sauk et al., 2005).

The modifications of collagen in the ER leads to the stability of the triple helix and is then secreted into the extracellular matrix. In the ECM, activated fibroblasts secrete an enzyme called lysyl oxidase (LOX) which belongs to the amine oxidase family and is hugely implicated in the crosslinking of extracellular matrix proteins including collagen and elastin. LOX and its family of lysyl oxidase like proteins (LOXL) are directly upregulated in activated myofibroblasts in the case of fibrosis and is responsible for the irreversible crosslinking of secreted collagens and thereby enabling their resistance towards MMPs. LOX is a copper dependent amine oxidase which uses carbonyl co-factor to covalently crosslink residues by oxidative deamination of several specific lysines and hydroxylysines. This leads to the formation of allysine and hydroxyallysine in the telopeptide domains of collagen. These crosslinks can further interact to form trivalent crosslinks making them extensively crosslinked in the ECM further strengthening their tensile properties. The crosslinked collagen can now act as trigger for activation of quiescent fibroblasts leading to further secretion of collagen and LOX and its LOXL family proteins to create a fatal feedback loop in fibrotic diseases. Therefore, targeting the activity of secreted lysyl oxidase (LOX) is a

promising approach towards the treatment of fibrotic diseases. β-aminopropionitrile (BAPN) is a lysyl oxidase inhibitor which irreversibly binds to the LOX active site thus preventing the formation of allysine and hydroxyallysine residues for crosslinking. BAPN was investigated for its function of decreasing several fibrotic conditions and in several forms of metastatic cancer where crosslinked collagen in the metastatic site serves as a favorable environment for colonization of migrated cancer cells (Smith-Mungo et al., 1998). Although LOX/LOXL inhibitors were effective in the animal models of fibrosis and metastasis, they failed to produce results in patients treated in multiple clinical trials. There is still a wide requirement for the pharmacological management of these diseases as current therapies prove ineffective, the search for new therapies with new mechanisms are being made one of which will be addressed in the form of PKM2 activators.

1.4 FIBROSIS

1.4.1 Wound Healing

Acute wound healing is characterized by four distinct overlapping phases. Hemostasis, inflammation, proliferation and remodeling. Acute wound healing beings immediately after the infliction of the wound. The first step of hemostasis occurs when the blood platelets, now exposed, binds with collagen present in the tissue matrix and are activated. Activated platelets secrete clotting factors to aid in the clotting of the blood to prevent more blood being spilled into the tissue. Along with the clotting factors, activated fibroblasts secrete an array of growth factors which include platelet derived growth factor (PDGF) and transforming growth factor – beta (TGF-□). Following hemostasis, inflammation phase occurs with the infiltration of neutrophils into the wound site. The neutrophils begin the process of phagocytosis and trigger the influx of macrophages. The infiltrated macrophages trigger a pro-inflammatory response and further

potentiate the release of TGF-β and PDGF. Macrophages carry out phagocytosis and clear the debris in the wound site. The next stage is the proliferative phase wherein the fibroblasts are activated due to the secretion of TGF-β and secrete new extracellular matrix. The secreted matrix is subsequently cross-linked which leads to the remodeling phase of wound healing.

Collagen is the most abundant protein in the animal kingdom. Collagen provides tensile strength, structure and integrity to tissues. During injury, the tissue integrity is compromised thereby requiring the replacement of collagen to repair the injury and regain tissue strength and integrity. Physiological wound healing is a dynamic process required for the restoration of tissue anatomy and function. This is achieved by the formation and remodeling of collagen-based scars in the tissue. The normal wound process involves the activation and secretion of collagen by fibroblasts and then they are either de-differentiated into quiescent fibroblasts or undergo apoptosis after tissue matrix remodeling. In the event of pathological wound healing, wherein the healing process of ECM deposition and tissue remodeling is not controlled, there is continued wound healing and continued infiltration of pro-inflammatory neutrophils and macrophages further enhancing inflammation followed by continued secretion and deposition of collagen by fibroblasts. These events collectively impair physiological wound healing and lead into a condition called fibrosis (Hernandez-Gea et al., 2011).

1.4.2 Fibrosis in Pathology

The pathological variant of tissue repair poses a stark difference from the inflammatory and secretory response observed in the physiological tissue repair. Typically, pathological wound healing is an extension of the healing process, leading to excessive and prolonged healing phase. In this phase, there in increased connective tissue deposition and this results in altered tissue structures and leads to loss of tissue function. Excessive wound healing manifests in several forms,

these include fibrosis, strictures, adhesions and contractions. During fibrosis, the fibroblasts are the main perpetuators of matrix deposition and tissue damage. During the proliferation phase of wound healing, TGF-□ secreted by the platelets, macrophages and T-lymphocytes initiate the activation of the fibroblasts to secrete ECM and is widely considered to be a master regulator of fibrosis. Increased TGF-□ signaling regulates fibroblast function is three distinct ways to facilitate wound healing, and in this case, excessive wound healing. First, it triggers the transcription of collagen and other ECM proteins through its SMAD-coSMAD pathway. This enables the fibroblasts to repair the wound site with the deposition of lost and damaged ECM. Parallelly, it also upregulates the secretion of matrix degradation enzymes called tissue inhibitors of matrix proteinases (TIMPs). These TIMPs inhibit the action of any secreted MMPs thereby reducing the degradation of the newly synthesized ECM. These effects in conjunction with each other facilitate the activation and subsequent wound healing properties of fibroblasts (Hata et al., 2016).

During the activation of these fibroblasts, there are several metabolic changes which occur within the fibroblasts. Upon activation, myofibroblasts are suddenly metabolically hyperactive thereby requiring an increased energy need to fuel the increased protein synthesis to secrete ECM and to survive the harsh conditions of the wound microenvironment. Herein, the fibroblasts are seen to produce more lactate which indicates the flux of glycolysis into lactate production pathway via the upregulation of lactate dehydrogenase A (LDHA) and pyruvate kinase M2 (PKM2). With the increased metabolic demand, there is an increased need for ATP to be generated, and with the glycolytic shunt towards lactate production, there is a dearth in the intermediates entering the citric acid cycle. Therefore, the activated fibroblasts upregulate their glutamine transporters. Upregulated glutamine is then converted in glutamate via glutamine synthetase (GLS). Glutamate can now be freely oxidized into alpha-ketoglutarate by glutamate dehydrogenase (GDH). □KG

can now enter the citric acid cycle and fuel the production of ATP. Therefore, the activated fibroblasts acquire glutamine dependency to fuel their altered metabolic state. During the high metabolic state, there is an increased requirement for oxygen, but the local wound microenvironment is a low-oxygen state which hinders the metabolic requirement for these fibroblasts. The low oxygen environment triggers the stabilization of HIF family proteins, leading to the upregulation of vascular endothelia growth factors (VEGF) in the surrounding endothelial cells. Increased VEGF in triggers neovascularization. This restores the flow of oxygen back into the wound site thereby aiding the metabolic demands of the fibroblasts for the secretion of collagen. Therefore, in fibrotic conditions, there is a marked upregulation of secreted lactate and HIF family proteins for an extended period. Secreted collagen can now be readily crosslinked with the secreted lysyl oxidase (LOX) family proteins. Crosslinked ECM components are not susceptible to degradation by MMPs and can further activate fibroblasts to secrete more ECM thereby promoting excessive wound healing leading to fibrosis. Pathological fibrosis is thereby a collection of signals and environmental triggers which culminate in the continued activation of quiescent fibroblasts leading to increased ECM deposition and leading to tissue damage (Herchenhan et al., 2015).

In the advent of fibrosis, there is a large influx of pro-inflammatory immune cells which are recruited into the wound site. There are several pro-inflammatory chemokines which facilitate the influx of these immune cells. The chemokines implicated in the perpetuation of fibrosis are broadly from the CC- and the CXC- family. The major mediators that facilitate the influx of mononuclear phagocytes which are the major pro-fibrogenic immune cells are CCL2 (monocyte chemoattractant protein-1) and CCL3 (macrophage inflammatory protein 1□). These chemokines attract the macrophage population which upregulate the secretion of several pro-

inflammatory interleukin family proteins such as IL-1□, IL4, IL-13 etc. IL-4 and IL-13 secreted by these cells can in turn upregulate the expression of CC- chemokine activity which leads to a positive feedback mechanism which exists to maintain this consistent pro-inflammatory condition in the wound site leading to consistent activation of fibroblasts. Apart from the chemokines, the chemokine receptors belonging to the CCR or the CXCR family also are implicated in the recruitment of pro-inflammatory macrophages into the wound site facilitating inflammation. Therefore, inflammation is widely considered to be a attractive target for the attenuation of fibrosis.

1.4.3 Hepatic Fibrosis

Liver fibrosis is a prime mediator of morbidity and mortality worldwide and can be facilitated due to several factors including but not limited to viral hepatitis, obesity associated fatty liver disease. The critical point in the fibrosis of the liver is the activation of hepatic stellate cells. Hepatic stellate cell injury is central for the fibrogenic response and for its secretion of ECM. Hepatic fibrosis is chronic wound healing in the hepatic parenchyma by the deposition of ECM by the activated hepatic stellate cells. Hepatic fibrosis is a reversible event. In the case of acute liver injury, the changes to the liver parenchyma is transient and the liver architecture is promptly restored to its normal composition. In the case of chronic liver injury, chronic inflammation persists and leads to the deposition of ECM in the liver parenchyma and forms scar tissue. The process of fibrosis upon further damage leads to liver cirrhosis which leads to poor outcome and increased morbidity and mortality. Progression of liver fibrosis into cirrhosis is generally very slow taking anywhere between 20 to 40 hours in patients with chronic liver injury. The hepatic parenchyma consists of a variety of cells which each perform specific functions. These cells types include hepatocytes which are liver epithelial cells and form most of the liver mass. Other cell

types include endothelial cells and resident non-parenchymal cells. These cells include hepatic stellate cells (HSCs) and Kupffer cells (KCs). HSCs are the resident fibroblasts in the liver whereas the KCs are the resident macrophages of the liver.

The hepatic vascular structures are arranged in a sinusoid-based structures. The endothelial cells form a lining of cells separated by fenestrations. The endothelial lining is separated from the hepatocyte epithelial bed by a sub-endothelial space known as the space of Disse. The hepatic stellate cells reside in the space of Disse. Hepatic stellate cells, in their quiescent state store vitamin A and upon activation loses its vitamin A stores and switches to a contractile, proliferative, secretory, metabolic and pro-fibrogenic myofibroblast like phenotype. Here, the environment is supportive for the maintenance and function of the parenchymal cells and is porous for the exchange of metabolites between the hepatocytes and the bloodstream. During liver injury, the hepatic stellate cells are activated and begin to secrete ECM in the space of Disse. Upon ECM accumulation, fenestrations that occur in the lining of the endothelial cells are now occluded which impairs the regular communication between the hepatocytes and the vascular bed. The occlusion of the sinusoids is called the capillarization of sinusoids. Sinusoid occlusion is a characteristic outlook of the progression of fibrosis. A major cause of liver fibrosis is chronic hepatitis B and hepatitis C which cause bridging fibrosis characterized by the presence of fibrotic septa. Fibrotic septa are formed by the interface hepatitis and portal-central vein bridging necrosis. Another major cause of fibrosis in the liver is related to the consumption of alcohol. Alcohol induced fibrosis is characterized by the deposition of ECM in the space of Disse around the sinusoids and hepatocytes. The other form of fibrosis is biliary fibrosis where there is an increased proliferation of bile ductules and periductular myofibroblasts. In biliary fibrosis, there is formation of fibrotic scars in the portal-portal septa which surrounds the liver nodules. Centrolobular fibrosis is mediated not

by the direct activation of fibroblasts but by the alteration of venous flow and is characterized by the central-central fibrotic septa.

ECM distribution in the normal liver is a dynamic process wherein the secretion and deposition of ECM and the degradation of the new ECM is carefully regulated by balancing the gap between generation and degradation. Liver fibrosis occurs when the deposition fraction exceeds the degradation factor and leads to increased accumulation of ECM leading to alteration of liver parenchyma and its function. The ECM is deposited and leads to the thickening of the fibrotic septa and is then chemically crosslinked. ECM in the liver is usually tightly organized that provides structural and functional integrity of the liver. The general distribution of ECM is relatively low at around 3% in a normal liver section and the usual composition is mainly collagen IV and VI. Collagen IV and VI are mesh-type collagens which form the support structures in the liver. During fibrotic injury, the deposition of collagen is mostly the fibrillar type collagen I and III. The altered type of ECM now deposited in the space of Disse is responsible for the alteration of the matrix microenvironment and creates a functional and physical impairment of the bidirectional communication between the vascular bed and the hepatocyte mass.

The presence of accumulated ECM in the liver during the fibrogenic response is responsible for the hardening of the liver parenchyma and induces the activation of fibroblasts. Apart from the physical implications of ECM, several growth factors bind to ECM and are preserved in their latent forms. Bound growth factors then facilitate the growth and maintenance of the local microenvironment and their cells. Decorin and biglycan can bind to TGF-□,□fibronectin and laminin bind to tumor necrosis factor □□(TNF-□), collagen binds to a variety of growth factors including platelet derived growth factor (PDGF), hepatocyte growth factor (HGF) and interleukin-12 (IL-12). ECM and the surrounded cells are bi-directional therefore ECM

can regulate the activation of HSCs, endothelial cells and the availability of growth factors lead to the accumulation of ECM and leads to a pro-fibrogenic positive feedback loop. Interaction of HSCs with the secreted ECM is determined by the receptor profile of the HSCs. The membrane receptors which interact with ECM are integrin family, a disintegrin and metalloproteinase domain (ADAM) molecules and several discoidin domain receptors. Integrins are critical for the activation of HSCs and are usually upregulated in activated HSCs hence promoting their binding to the surrounding ECM. ADAMSTS-1 and ADAMSTS-13 are expressed by the endothelial cells and activated HSCs respectively. Discoidin domain receptor 2 (DDR2) potentiates HSC activation. Secretion of collagen I induces DDR2 phosphorylation leading to increased MMP2 production.

TGF-β is the major cytokine responsible for the activation of HSCs in the liver. TGF-□ is secreted by various cell types and in different isoforms TGF- β 1, TGF- β 2 and TGF- β 3. TGF- β 1 is mainly secreted by macrophages and monocytes and TGF- β 1 is the principal isoform which is implicated in the progression of liver fibrosis. TGF- β 1 is stored as an inactivate protein bound to another latency associated protein. Upon activation, TGF- β 1 binds to its receptor TGF β R2 and dimerizes with TGF β R1 and binds to SMAD2 and SMAD3 and this complex is now phosphorylated and binds to its co-SMAD, SMAD4. This complex translocates into the nucleus resulting in the transcription of procollagen 1 and procollagen 3. Therefore, TGF- β is a direct responsible cytokine in the initiation and the progression of collagen in the advent of liver fibrosis.

Given the pathology of liver fibrosis, several studies have been carried out to test the reversibility of fibrotic insult. Fibrosis of the liver can be reversed by several approaches. Direct removal of the causative agent has shown to be critical in the resolution of fibrosis in several animal models. In other cases of a persistent underlying cause for the progression of fibrosis, the removal of the underlying cause, like resolution of hepatitis B or C viral infection, lead to the

resolution of disease induced fibrosis. In alcohol induced fibrosis, removal of alcohol from the diet lead to the quick resolution of fibrosis. The mechanisms behind resolution of fibrosis are linked to some for of degradation of the ECM. ECM is a dynamic balance between its generation and degradation. ECM degradation is carried out by matrix metalloproteinases. MMPs are regulated in the liver at various levels. They are tightly transcriptionally controlled and secreted as inactive pro-enzymes. To restrict their enzymatic activity, tissue inhibitors of matrix metalloproteinases (TIMPs) are secreted and bind to all the MMP isoforms and thus control their degradation activity. TIMP family proteins play a major role in the alleviation of liver fibrosis. TIMP-1 plays a role in the apoptosis of HSCs and since HSCs are the major source of MMP-2, MMP-3, MMP-9 and MMP-13, their removal impairs the progression of liver fibrosis. HSC depletion is critical to the resolution of fibrosis and it is carried out by several mechanisms which include the inactivation of NF-kB and thereby reducing its survival signaling. Immune cells such as NK cells can also induce HSC apoptosis by expression of TRAIL ligand which can directly bind to HSCs and induce apoptosis. Several components of ECM can also lead to apoptosis if their binding to their respective ECM receptors on HSCs is abrogated such as integrin □3□2 which increases the ratio of Bax/Bcl2 and induces caspase 3 activation in HSCs. Therefore, hepatic fibrosis is a dynamic and complex process which is regulated in several ways by tightly controlled pathways and can lead to hepatic cirrhosis which is the leading digestive disease which causes death. And the resolution of fibrosis is a challenge and new therapies and targets are required to ameliorate fibrosis and reduce morbidity and mortality (Hernandez-Gea et al., 2011).

1.4.4 Pulmonary Fibrosis

In many pulmonary diseases, the end stage results in the formation of fibrotic scars in the lung called pulmonary fibrosis. Pulmonary fibrosis is characterized by the excess accumulation of

extracellular matrix which leads to the compromise of pulmonary structure and function. This eventually leads to difficulty breathing and finally death. The most common type of pulmonary fibrosis is idiopathic pulmonary fibrosis (IPF). IPF is a widespread disease with a very low 5-year survival rate of 20% which leads to the requirement of immediate therapeutic options for treatment. Lungs affected with IPF characteristically show alternating fibrotic regions, normal lung parenchyma, followed by alternating inflamed regions and fibrotic regions and honeycombing. The advent of lung fibrosis is usually through response to acute injury in the multi-focal epithelium. Repeated injury to the micro epithelium results in the apoptosis of alveolar epithelial cells. This impaired alveolar epithelium results in aberrant interactions between the epithelial cells and the fibroblasts of the lung and therefore lead toward impaired healing processes. The healing cascade in the lung is usually tightly controlled and regulated by many cell signaling events and homeostasis of the lung epithelial ECM components. The impaired healing processes lead to uncontrolled healing signals leading to accumulation of excessive extracellular matrix in the lung parenchyma leading to pulmonary fibrosis.

Several potential causes have been isolated for the initiation and propagation of IPF. Some of them include immunological disorders, oxidative stress mediated apoptosis, endoplasmic reticulum stress, coagulation cascade proteins, and even the possible role of stem cells are studied. Even though many possible avenues have been studied to identify the etiology of pulmonary fibrosis, the direct role of specific agents to initiate fibrosis remains unclear. In general, initiation of fibrosis is observed when there is repeated injury which would lead to the apoptosis of the alveolar epithelial cells. A genetic pre-disposition is generally suspected due to the associated SP-A and SP-AC mutations in the alveolar epithelium. These mutations lead to a dysfunctional epithelium leading to disrupted alveolar epithelium homeostasis leading to a fibrotic trigger.

Several environmental triggers have also been isolated which are implicated in the repeated injury to the alveolar epithelium. Inhaled injurious agents trigger a pro-inflammatory response in the lungs. The immune response to the inhaled agents triggers a similar response as a repeated injury and can trigger the fibrotic cascade. Similar to the liver, virus based infections lead to repeated insult and injury to the epithelium leading to fibrosis. In the case of lungs, the major viral agent is the Epstein-Barr virus (EBV), several other viral infections have since been identified namely herpes simplex virus 7 and 8, parvovirus B19, torque teno virus and several cytomegaloviruses. The most widely implicated virus, the EBV, triggers an immune response which enables the influx of pro-inflammatory neutrophils, monocytes and macrophages which are all a major source of TGF-β. TGF-β is known to interact with EBV and potentiate viral lytic phase activation and resistance to inhibition of growth.

Recurrent injury to the pulmonary epithelium leads to the damage of the alveolar capillary basement membrane. This enables an influx of fibroblasts which are consequently activated by the immune cell secreted TGF-β into myofibroblasts. These myofibroblasts secrete excessive ECM leading to the destruction of lung parenchyma and loss of lung function. Lung fibroblasts proliferate due to the production of fibroblast growth factor-2 which activates the MAPK pathway leading to increased fibroblast population and TGF-β can activate them to begin the fibrotic wound healing cascade. As seen in the liver, the recruitment of the initial pro-inflammatory mediators is mediated by the CC- and CXC- family of chemokines. Inn the lung, CCL2 and CCL3 are the most implicated which act via their respective receptors, mainly CCR2.

Like the fibrotic processes in the liver, the fibrogenic process in the lungs is the imbalance between ECM secretion and ECM degradation. ECM in the lungs is degraded by MMPs secreted by myofibroblasts. These myofibroblasts also secrete TIMPs which can reversibly inhibit the

activity of MMPs and lead to decreased ECM degradation. The deposited ECM can now be chemically crosslinked by the LOX family proteins which are secreted by the myofibroblasts. These covalently crosslinked ECM, mainly collagen I, is resistant to the action of MMPs and leads to the collapse of the alveolar structures and decline in the lung function. The general cascade of events in the lungs is like the liver wherein there is an initial and repetitive insult and injury. In the lungs, epithelial damage leads to endothelial damage of the alveolar capillary basement membrane thereby reducing the structural integrity. The absolution of the basement memory leads to vascular leaks. Vascular leaks trigger the coagulation cascade in the platelets notably the secretion of PDGF. The release of PDGF triggers the proliferation of the resident lung fibroblasts. The presence of PDGF also leads to the influx of macrophages which trigger secretion of TGF-β and myofibroblast activation. The fibrogenic response leads to the deposition of ECM and the presence of repeated injury leads to the consistent activation of the myofibroblasts which leads to exaggerated ECM accumulation, lack of ECM degradation, progressive ECM remodeling and honeycomb changes. These cascade of events leads to the loss of lung function and eventually, death.

The current treatment options for the treatment of IPF still revolves around resolution of the persistent inflammation present in the lung epithelium. To tackle this phenomenon, anti-inflammatory agents are still the standard treatment option for IPF. Since the underlying cause in IPF is usually unknown and the resolution of ECM secretion is not checked, the need for novel therapeutic options is still a major area for drug development (Wuyts et al., 2013).

2 METHODS AND MATERIALS

2.1 CELL CULTURE

2.1.1 Growth and maintenance

LX2 cells were obtained from Millipore (Cat#SCC064) and NLF cells were obtained from Lonza (Cat#) and were maintained in DMEM (Corning Cat#10-013) supplemented with 2% FBS and 1% penicillin-streptomycin solution (Corning Cat# 30-002CL). Cells were maintained in a 37C incubator in 5%CO_2 for all treatments listed.

2.1.2 Growth factor treatment

To activate the fibroblasts, TGF-β(R&D systems Cat# dissolved in PBS was added at 10ng/mL and incubated for 48 hours in DMEM supplemented with 2% FBS and 1mM glutamine (Corning Cat#25-005CL).

2.1.3 PKM2 activator treatment

PKM2 activator DASA-10 was obtained from Millipore (Cat# 550602) and was dissolved in DMSO to make a stock concentration of 10mM. DMSO or DASA-10 was added to the activated fibroblasts at a final concentration of 10µM for 24 hours or 48 hours wherever specified.

2.1.4 RNA interference

SiRNA for PTBP1 was purchased from Santa Cruz (Cat# SC-38280) and was diluted with water to make a stock concentration of 100µM. RNA iMAX was purchased from Thermo(Cat # 13778030) and Opti-MEM was purchased from Thermo (Cat# 11058021). SiRNA was diluted in 250µL of Opti-MEM to achieve a final amount of 10pmol. 5µg of RNA iMAX was diluted in 250µL of Opti-MEM and they were combined and incubated for 20 minutes. The mixture was then

added to the cells and incubated for 4 hours. Cells were then supplemented with DMEM for 24 hours and analyzed for RNA interference with a western blot.

2.2 Western blot

2.2.1 Whole cell lysate preparation

10x RIPA lysis buffer was purchased from Millipore (Cat# 20-188). 1X RIPA buffer was prepared with 1X protease and 1X phosphatase inhibitors. Cell pellets were lysed in the lysis buffer for 30 minutes at 4C and centrifuged at 14000 rpm for 10 minutes. The supernatant was stored in -80C. Protein concentration was measured using Bradford assay (BioRad Cat#5000201).

2.2.2 SDS PAGE and immunoblot

30µg of lysate was subjected to gel electrophoresis on a 10% SDS gel until the target protein molecular weights were resolved and transferred to nitrocellulose membrane at 120mAmps for 2 hours. Membranes were blocked with 5% milk for 1 hour and probed with one of the following antibodies overnight at 4C. Antibodies used were either Anti-rabbit or anti-mouse. PKM2 (Cell Signaling, Cat# 4053S, 1:1000), PHGDH (Cell Signaling Cat# 66350S, 1:1000), □-SMA (Cell Signaling Cat# A5228, 1:1000), □-actin (Yurogen Cat# R15006MC4H, 1:10,000). HRP conjugated anti-rabbit (Thermo cat# 31460, 1:10,000) or anti-mouse (Thermo Cat# 31430, 1:10,000) were used based on the primary antibodies. Membranes were developed with ECL substrate purchased from Thermo (Cat# 32106).

2.3 Reverse transcriptase-polymerase chain reaction

2.3.1 RNA Isolation

RNA was isolated from cells and tissues using Tri reagent (Cat# 15596026) with the provided manufacturer's protocol. In brief, cells were lysed in Tri reagent and extracted with

chloroform and centrifuged at 14000 rpm for 15 minutes. Isopropanol was added to the top aqueous layer and centrifuged at 14000 rpm for 15 minutes. The precipitated RNA pellet was then washed with 75% ethanol. The RNA pellet was then dissolved in water and stored at -80C.

2.3.2 Reverse Transcription

RNA was measured with a NanoDrop and 2µg of RNA was used for cDNA conversion using MAXIMA cDNA first strand synthesis kit purchased from Thermo (Cat# K1641) using the manufacturer's protocol. In brief, RNA was measured and was added to the enzyme mix and cycled in the following parameters: 25C for 10 minutes, 50C for 15 minutes, 85C for 5 minutes. The resultant mixture was diluted to 200µL and 5mL was used for qPCR analyses.

2.3.3 qPCR

qPCR was carried out using LUNA qPCR SYBR GREEN mastermix was purchased from NEB (M3003L) in a Thermo 7500 Fast qPCR machine. The primers were purchased from Thermo and are listed in Table 1. These primers were diluted to a stock concentration of 100µM and were re-diluted to a working concentration of 10µM. 5µL of the prepared cDNA, 0.5µL of each forward and reverse primers, and 5µL of the provided mastermix were run through the qPCR thermocycler for 40 cycles. The resultant threshold cycles for the genes were analyzed using the ΔΔCT method.

2.4 Immunohistochemistry

Formalin fixed paraffin embedded were sectioned at 5µm thickness and mounted onto charged slides. Immunochemistry kit was purchased from (BioCare Cat# M2U522) was performed on these slides using manufacturer's protocol. Briefly,slides were baked in a 60C oven for 2 hours. They were washed with TBST followed by protein and peroxide block. The slides were incubated with primary antibodies at various concentrations depending on manufacturer's protocol. The

slides were then washed and probed with HRP-conjugated polymer. DAB and its substrate were used to stain the polymer.

2.5 Immunofluorescence

Tissues were rinsed in PBS and processed through serial dilutions of sucrose (10%, 15% and 30%) before embedding in OCT (Tissue-Tek) and then immediately frozen in liquid nitrogen. 10-μm thick sections were washed with PBS, fixed in acetone and incubated with primary antibodies overnight. Alexa Fluor 488 and 555 secondary antibodies were used to visualize IF staining. Nuclei were counterstained with DAPI. Images were taken using a Keyence microscope camera and analyzed using Adobe Photoshop CS6. The following antibody dilutions were used: αSMA, 1:200 (#A5228, Sigma Aldrich); PKM2, 1:500 (#4053, Cell Signaling Technology), Cleaved Caspase 3, 1:500 (#9661, Abcam); CD68, 1:500 (#125212, Abcam).

2.6 High pressure liquid chromatography

2.6.1 Sample preparation

$1x10^6$ cells were used for all HPLC analyses. Cells were washed with 0.9% NaCl and flash fixed in precooled 50% methanol. The cells were then scraped and transferred to an Eppendorf tube. Chloroform was added to the samples and were lysed for 30 minutes at 4C. The lysates were centrifuged at 14000 rpm for 10 minutes and the aqueous phase was used for amino acid analyses.

2.6.2 Reversed Phase liquid chromatography

Amino acid standards were purchased from Sigma (Cat# AAS18). Amino acids were then derivatized with phenylisothiocyanate (PITC) purchased from Sigma (Cat# 26922). Derivatized samples were analyzed using a reversed phase HPLC Agilent system (1260 Infinity II). Agilent C_{18} 150mm column (Agilent Poroshell 120) was used to resolve the amino acids and were analyzed by a UV-DAD detector at 254nm.

2.7 Liquid chromatography mass spectrometry

Acetonitrile (LCMS grade), water (LCMS grade) and formic acid (LCMS grade) were purchased from Fisher Scientific. LC-MS/MS analysis was carried out with a Sciex API3200 esi-triple quandrupole mass spectrometer coupled with an Agilent 1200 HPLC. A Phenomenex Germini NX-C_{18} column (3 µm, 100x3mm) was used with flow rate of 200µL/min. Mobile phase was 1% ACN containing 0.1% HCOOH (mobile phase B) and 99% water containing 0.1% HCOOH (mobile phase A). The analysis was isocratic for 10 min. 5µL of each standard and sample was injected into the system. The MS ion source used was esi in a positive selective reaction mode (SRM) with the precursor/product ion pairs listed in the following table. The MS parameters used are as follows: Ion source (IS) voltage, 5400 v, ion source temperature 450C, collision energy 5v. Analyst 1.5.1 was used for data analysis.

2.8 Size exclusion chromatography

Cells were lysed and total protein was extracted with RIPA. 2mg of cellular protein was separated using a HiPrep 16/60 Sephacryl S-200 HR columns in 50mM sodium phosphate and 150mM codium chloride, pH 7.2. Fractions were collected and analyzed at UV 280nm.

2.9 Induction of liver fibrosis

For the induction of liver fibrosis, the thioacetamide (Fisher Cat# AC424530250) (TAA)-ethanol model of liver fibrosis was used. In short, BALB/cJ mice aged 6 weeks were provided with 10% ethanol in drinking water *at libitum* and TAA was administered at 100mg/Kg i.p. bi-weekly for 5 weeks. The dose was increased to 250mg/Kg for another 7 weeks. Mice were treated with TEPP-46 (insert cat) at 50 mg/Kg daily for 21 days. Mice were euthanized in a CO_2 chamber and tissues were harvested for further analysis.

2.10 Induction of lung fibrosis

For the induction of lung fibrosis, the bleomycin (Selleckchem Cat# S1214) model of lung fibrosis was used. In short, C57/BL mice aged 6 weeks were administered with 4mg/Kg bleomycin i.p. bi-weekly for 4 weeks. Mice were treated with TEPP-46 at 50mg/Kg daily for 21 days. Mice were euthanized in a CO_2 chamber and tissues were harvested for further analysis.

Table 1 List of primers

Gene	Sequence (5'-3')
Human	
hPHGDHF	GGAGGAGATCTGGCCTCTCT
hPHDGHR	GTCATTCAGCAAGCCTGTCG
hPSPHF	GGACTCCCTTTTAAGCAGATCTCA
hPSPHR	TTCCCAGGGAGGTGAGCTG
hPSAT1F	GCGGCCATGGAGAAGCTTAG
hPSAT1R	ATGCCTCCCACAGACACGTA
hSHMT1F	GTGACCACCACCACTCACAA
hSHMT1R	ACAGCAACCCCTTTCCTGTAG
hSHMT2F	GCTGCCCTAGACCAGAGTTG
hSHMT2R	GCAGAGGCCGAGCCG
hCOL1A1F	GGTCAGATGGGCCCCCG
hCOL1A1R	GCACCATCATTTCCACGAGC
hPKM2F	ATTATTTGAGGAACTCCGCCGCCT
hPKM2R	ATTCCGGGTCACAGCAATGATGG
hActinF	CTCGCCTTTGCCGATCC
hActinR	TCTCCATGTCGTCCCAGTTG
Mouse	
mCCL2F	TTTTGTCACCAAGCTCAAGAGA
mCCL2R	ATTAAGGCATCACAGTCCGAGT
mIL1bF	CCAAAAGATGAAGGGCTGCT

mIL1bR	ACAGAGGATGGGCTCTTCT
mIL6F	GAGGATACCACTCCCAACAGACC
mIL6R	AAGTGCATCATCGTTGTTCATACA
mIL10F	ATAACTGCACCCACTTCCCA
mIL10R	GGGCATCACTTCTACCAGGT
m18sF	CGCTTCCTTACCTGGTTGAT
m18sR	GAGCGACCAAAGGAACCATA
mActinF	AGTGTGACGTTGACATCCGT
mActinR	GCAGCTCAGTAACAGTCCGC

3 PYRUVATE KINASE IN FIBROSIS

3.1 Abstract

Fibrosis is a pathological condition that is associated with the accumulation of excess collagen in the extracellular space by activated myofibroblasts. Activated myofibroblasts upregulate Pyruvate Kinase M2 which reduces the production of pyruvate and leads to accumulation of glycolytic intermediates. Glycolytic intermediates feed into several anabolic processes including glycine synthesis. Glycine is required to produce collagen strands to secrete collagen because it is an essential part of collagen's XaaYaaGly motif. The demand of glycine is satisfied by both transport into the cell and *de novo* synthesis. We utilized a PKM2 activator to upregulate glycolysis and deplete its intermediates therefore reducing the flux to glycine synthesis. PKM2 activator treatment reduced the production of glycine and collagen in these fibroblasts and reduced the progression of fibrosis in liver and lung.

3.2 Introduction

Fibrosis is a condition wherein excess collagen is accumulated in the extracellular matrix by specialized set of cells. The cells which are responsible for the secretion of collagen are called myofibroblasts. Quiescent fibroblasts do not have the ability to secrete collagen. For them to differentiate into myofibroblasts, they must be activated. Quiescent fibroblasts are activated by TGF-β secreted by infiltrating macrophages in response to liver injury. In the liver, these quiescent fibroblasts are called hepatic stellate cells (HSCs). Upon exposure to TGF-β, HSCs get activated and are differentiated into myofibroblasts. The activation of HSCs lead to secretion and accumulation of collagen in the liver leading to liver fibrosis. The activation of fibroblasts leads to the upregulation of pyruvate kinase M2 by alternate splicing. PKM2 is an isoform of PKM gene which is responsible for the final step of glycolysis. PKM1 is a consistently active isoform and

provides constant movement of pyruvate into the citric acid cycle. PKM2 on the other hand can be regulated into its dimer and tetramer states by various posttranslational modifications including phosphorylation, succinylation etc. Dimer PKM2 is its inactive state and has a low glycolytic index. This leads to the accumulation of glycolytic intermediates and can channel 3-phospho glycerate (3PG) into *de novo* serine and glycine synthesis. Glycine is an integral part of the collagen fibril. Collagen is primarily made of a repeating triple amino acid motif usually in the XaaYaaGly sequence. Therefore, activated fibroblasts can upregulate *de novo* glycine synthesis to fuel its need for collagen production. Activation of PKM2 using synthetic activators, DASA-10 and TEPP-46, impairs glycine synthesis by shunting the intermediates into the citric acid cycle. The reduced reserves of glycine impair collagen synthesis by these fibroblasts. The usage of metabolic activators to inhibit collagen synthesis is a novel approach to tackle fibrotic diseases.

3.3 Results

3.3.1 PKM2 is upregulated in fibrotic tissues

In the event of fibrosis, tissues have been known to activate their resident quiescent fibroblast populations into a more active myofibroblast phenotype. The myofibroblast marker is a variant of smooth muscle actin called alpha smooth muscle actin (αSMA). We procured human liver and lung fibrotic tissue arrays from USBIOMAX and immunostained them with PKM2 to signify the areas where the activation of these fibroblasts is prevalent. We stained similar areas with Sirius Red for the presence of collagen. We observed that the localization of the immunostain and the Sirius red stain was contained to the stromal region of these tissues (Figure 3-1A). To test this in an *in vitro* system, we treated hepatic stellate cells (LX2) and normal lung fibroblasts (NLF) with 10ng/mL of TGF-β to activate these fibroblasts. Cells were activated for 48 hours and were lysed for RNA analyses. RT-PCR was performed on the samples and several genes related to

myofibroblast phenotype were measured. PKM2, αSMA and COL1A1 were measured in LX2 cells (Figure 3-1B) and in NLF cells (Figure 3-1C). After treatment with TGF-β for 48 hours, αSMA, PKM2 and COL1A1 genes were significantly upregulated leading to a myofibroblast like phenotype. 30µg of protein was loaded and immunoblotted for αSMA, PKM2 in the inactivated and activated LX2 and NLF cells to test the upregulation of myofibroblast like phenotype (Figure 3-1D). The protein profile of the activated fibroblasts is a direct representative of their mRNA profile in that PKM2 is upregulated by around 1.5-fold in activated LX2 along with αSMA whose fold change is around 1.5. In activated NLF cells, the fold change of PKM2 is also around 1.5-fold but αSMA had a higher fold change (Figure 3-1 E&F).

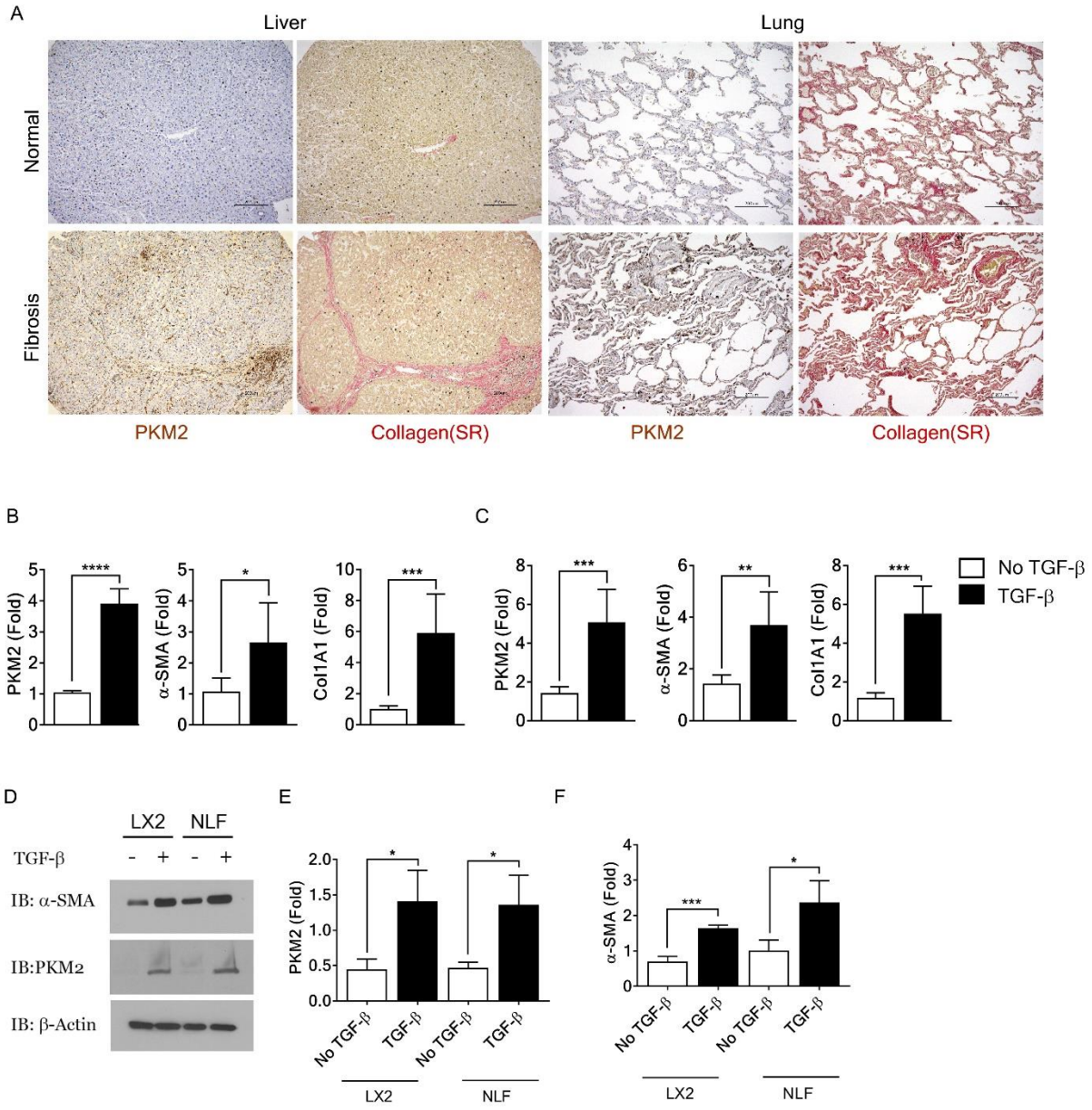

Figure 3-1 PKM2 is upregulated in fibrotic tissues and in activated fibroblasts.

(A)Tissue microarrays for healthy and fibrotic lungs and livers were probed with PKM2 and collagen 1 and were found to be localized to the stromal region in human fibrotic liver and lung. (B) RT-PCR analyses of inactivated and activated hepatic stellate cells (LX2) for PKM2, αSMA and COL1A1. (C) RT-PCR analyses of inactivated and activated normal lung fibroblasts (NLF) for PKM2, αSMA and COL1A1. (D) Inactive and active LX2 and NLF cells were lysed and 30µg

of lysates were immunoblotted for αSMA and PKM2. (E,F) Quantification of the fold increase of αSMA and PKM2 in LX2 and NLF cells respectively.

3.3.2TGF-β promotes Warburg effect

We observed that the expression of PKM2 and αSMA was consistent in response to TGF-β treatment. PKM2 exhibits low glycolytic activity in comparison to PKM1. The low glycolytic index leads to the accumulation of the intermediates of glycolysis. Glycolytic intermediates are usually shunted into several anabolic processes which include the pentose phosphate pathway (PPP), *de novo* serine and synthesis etc. To analyze the flow of these intermediates, we tested for the levels of several glycolytic intermediates in activated LX2 and NLF cells. In LX2 cells treatment with TGF-β increased the accumulation of glucose-6-phosphate (G6P) considerably from an average of 80μM to 95μM (Figure 3-2A). We also assessed the accumulation of 2-phosphoglycerate (2PG), another glycolytic intermediate, who's upstream 3-phosphoglycerate leads to the synthesis of serine. We observed that 2PG was also significantly accumulated in these cells (Figure 3-2B). We then proceeded to test whether the upregulation of PKM2 by TGF-β lead to the reduction of pyruvate kinase activity in the activated LX2 cells. Evidently, the addition of TGF-β, lead to a stark reduction in PK activity (Figure 3-2C). This reduction of PK activity directly correlates with the accumulation of G6P and 2PG in these cells. We next asked whether the effect of lowered PK activity and accumulation of the intermediates leads to *de novo* serine and subsequent glycine synthesis. We employed an LC/MS approach to determine the quantity of serine (Figure 3-2D) and a fluorometric determination of glycine quantity (Figure 3-2E). The levels of both serine and glycine have considerably increased in these cells post activation. We wanted to test whether a similar phenomenon could be observed in activated NLF cells, as they showed an upregulation of PKM2 along with αSMA. In keeping with the levels of the

intermediates in LX2 cells, NLF cells also showed increased G6P accumulation (Figure 3-2F), increased 2PG accumulation (Figure 3-2G) and decreased PK activity (Figure 3-2H). We then tested whether *de novo* serine and glycine synthesis were also affected in NLF cells and evidently, both serine and glycine levels were considerably increased upon activation of NLF cells. Activated myofibroblasts are the main source of collagen in fibrotic tissues. Therefore, to test the levels of collagen produced in these cells upon activation, we tested the levels of hydroxyproline, an amino acid exclusive to collagen, in these cells We observed that in both LX2 (Figure 3-2I) and NLF (Figure 3-2F), the levels of hydroxyproline significantly increased.

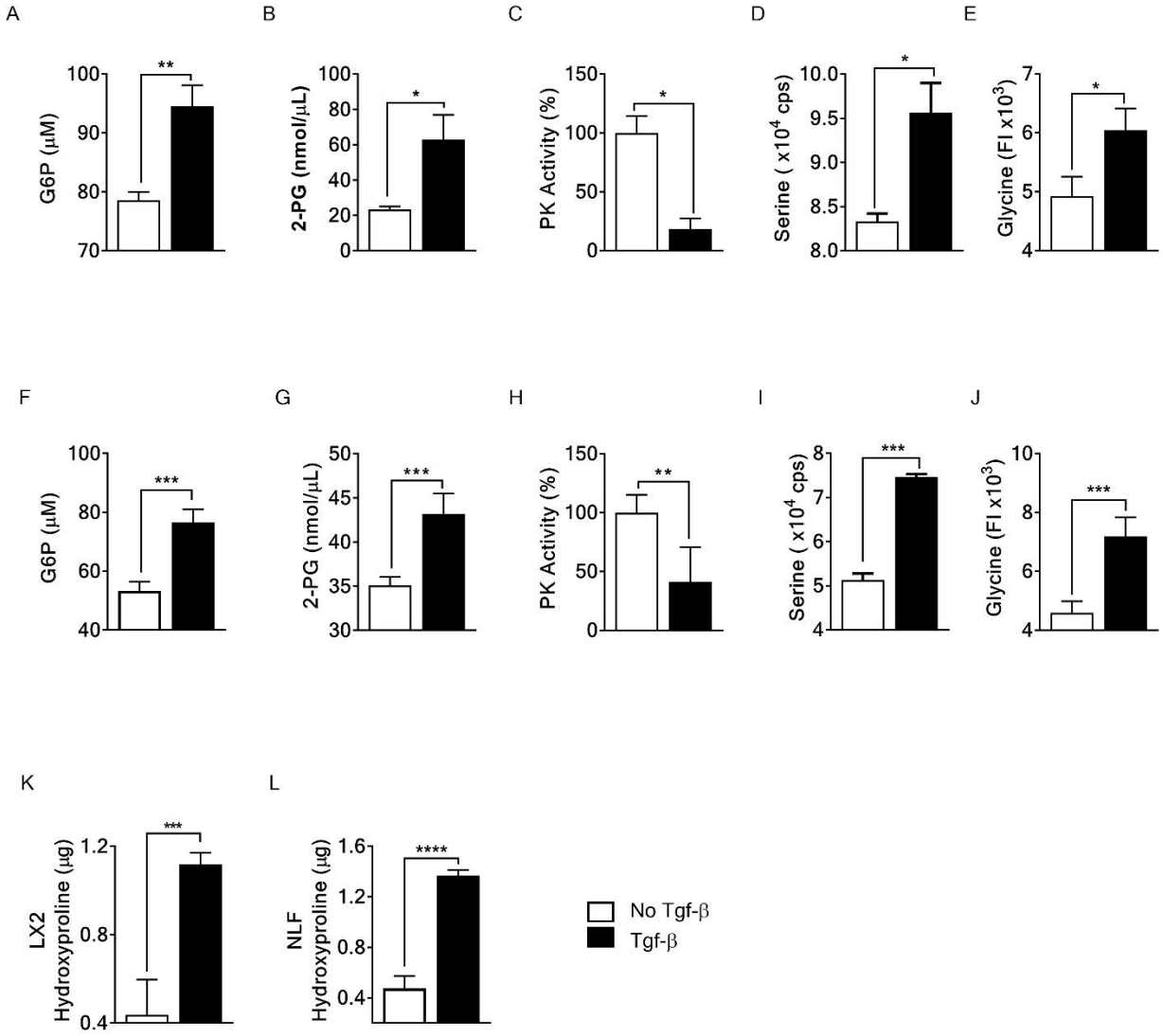
A
B
C
D
E
F
G
H
I
J
K
L
G6P (μM)
2-PG (nmol/μL)
PK Activity (%)
Serine (x10^4 cps)
Glycine (FI x10^3)
LX2 Hydroxyproline (μg)
NLF Hydroxyproline (μg)
No Tgf-β
Tgf-β

Figure 3-2 TGF-β promotes Warburg effect in hepatic stellate cells (LX2) and normal lung fibroblasts (NLF)

$5x10^5$ LX2 cells were used in the measurement of glycolytic intermediates, (A) G6P and (B) 2PG using a G6P (BioVision Cat#K657) and 2PG (BioVision Cat#K778) detection kits. (C) The PK activity was measured in these cells using a PK activity assasy kit (BioVision Cat#K709). (D) Serine levels were measured with LC/MS. (E) Glycine levels measured with a glycine assay kit (Abcam Cat#AB211100). $5x10^5$ NLF cells were used in the measurement of glycolytic intermediates, (F) G6P and (G) 2PG. (H) PK activity was measured as before. (I) Serine levels were measured as mentioned before. (J) Glycine levels were measured as mentioned before. The assay kits used in the detection of G6P, 2PG, PK activity and glycine levels were the same for LX2 and NLF. Serine was measured in both LX2 and NLF cells using LC/MS as described in the methods. Hydroxyproline was tested in (K) LX2 and (L) NLF cells using a hydroxyproline detection kit (Sigma Cat#MAK008). All cells were either treated with PBS (clear bars) or 10ng/mL of TGF-β for 48 hours (filled bars).

3.3.3TEPP-46 reverses liver fibrosis

The capacity of PKM2 activators to activate glycolysis by 200% was observed in activated liver stellate cells. With the increased activity of PKM2, the glycolytic intermediates were depleted rapidly thereby removing the intermediates necessary for *de novo* serine and further glycine synthesis. The halting of *de novo* serine and glycine synthesis lead to decreased collagen synthesis *in vitro*. During a fibrotic injury the hepatic stellate cells are activated and leads to secretion of collagen into the hepatic extracellular space. This accumulation of pathological collagen leads to liver fibrosis and eventually to liver cirrhosis. We wanted to test whether this phenomenon can be observed *in vivo* in a model of alcohol induced liver fibrosis. To induce liver injury, the

thioacetamide (TAA)-ethanol model was used. 10% ethanol in drinking water was provided to Balb/cJ mice and were administered with TAA for a period of 12 weeks followed by 7 weeks of treatment with TEPP-46 (Figure 3-3A). After the end of treatment, animals were sacrificed, and livers were photographed to identify gross structural differences if any. The gross images of both vehicle and TEPP-46 treated groups show significant differences in their surface morphology (Figure 3-3B). On the surface of the livers in the vehicle group, collagen accumulation can be observed in the form of white spots, whereas in the TEPP-46 treated livers show morphology like a normal liver. We then analyzed the aspartate aminotransferase (AST) and alanine aminotransferase (ALT) in the serum of these mice. The levels of AST (Figure 3-3C) and ALT (Figure 3-3D) were significantly lowered in the treated group which indicates improved liver function and decreased liver damage. We then tracked the weights of the animals during the treatment phase and in the TEPP-46 treated group, gained weight drastically within a week of treatment whereas the vehicle group continued deterioration (Figure 3-3E). We then proceeded to examine the collagen accumulation in the liver parenchyma. We stained the livers from both vehicle and TEPP-46 groups for collagen using Sirius Red stain. The stained area of collagen was quantified, and the mice treated with TEPP-46 have reduced collagen accumulation in the liver extracellular area (Figure 3-3F). Since most of the collagen is secreted by myofibroblasts, we stained the livers with αSMA antibody to assess the spread of myofibroblasts within the tissue. The TEPP-46 treated group show lowered levels of αSMA positive cells which denotes that the treatment has depleted a few myofibroblasts in the liver (Figure 3-3G). We then assessed the levels of PKM2 using immunofluorescence and there was no considerable difference between the vehicle and the TEPP-46 groups (Figure 3-3H). As the mice showed gross increase in body weight coupled with lowered AST/ALT levels and reduced collagen and αSMA in the treated group, we wanted

to verify whether the treatment had any effects on the free amino acid profiles of the liver. We analyzed the liver lysates with LC/MS for all amino acids and observed almost no difference in their levels barring a few amino acids (Figure 3-3I). We then turned our attention towards serine and glycine levels in these livers and indeed the levels of serine (Figure 3-3J) and glycine (Figure 3-3K) were decreased in the treated group thereby providing evidence that the lack of *de novo* serine and subsequent glycine synthesis lead to the lower collagen production and accumulation in the treated livers.

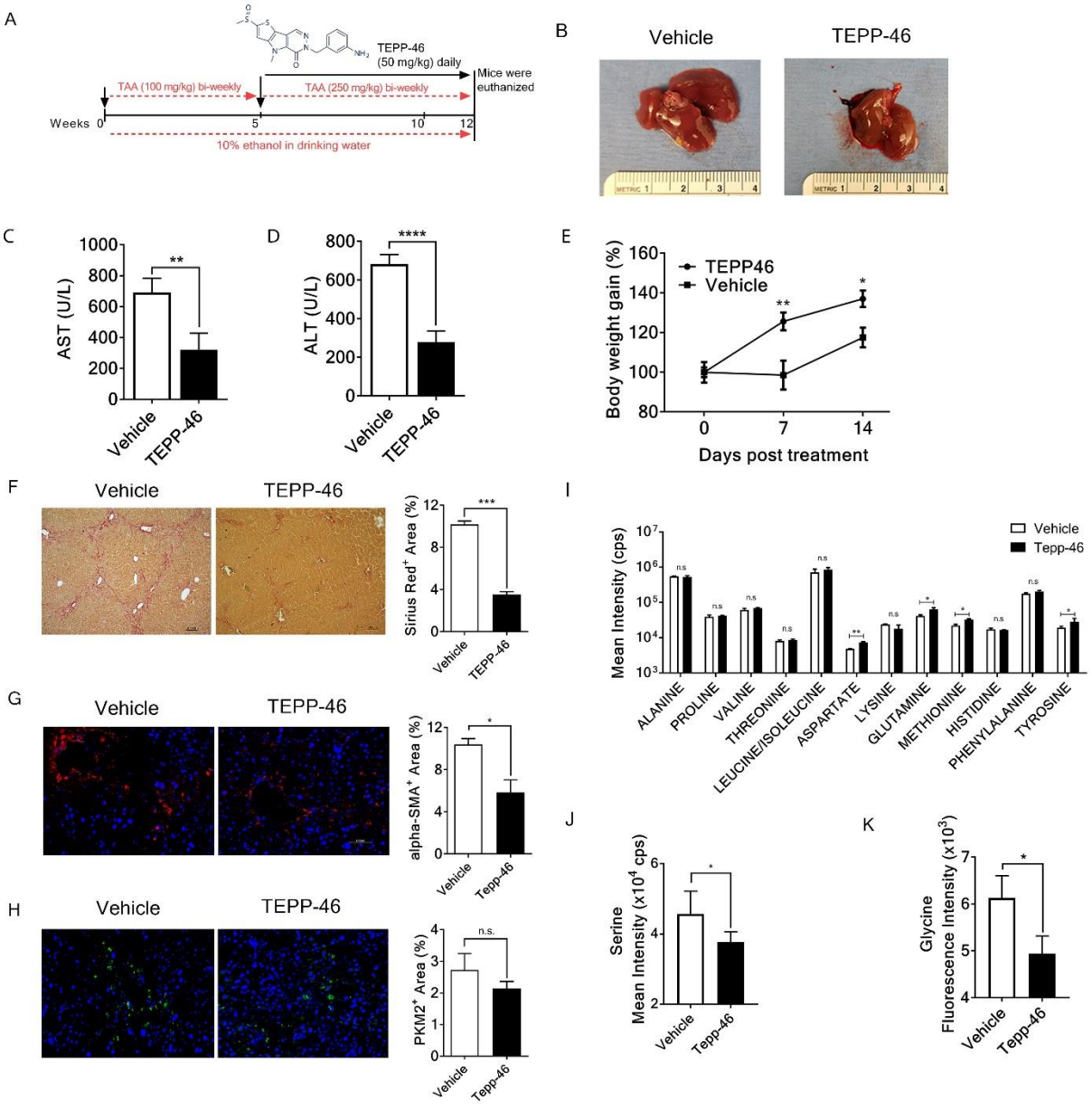
A
TEPP-46
(50 mg/kg) daily
TAA (100 mg/kg) bi-weekly
TAA (250 mg/kg) bi-weekly
Mice were euthanized
Weeks 0
5
10
12
10% ethanol in drinking water
B
Vehicle
TEPP-46
C
AST (U/L)
Vehicle
TEPP-46
D
ALT (U/L)
Vehicle
TEPP-46
E
TEPP46
Vehicle
Body weight gain (%)
Days post treatment
F
Vehicle
TEPP-46
Sirius Red+ Area (%)
G
Vehicle
TEPP-46
alpha-SMA+ Area (%)
H
Vehicle
TEPP-46
PKM2+ Area (%)
I
Vehicle
Tepp-46
Mean Intensity (cps)
ALANINE
PROLINE
VALINE
THREONINE
LEUCINE/ISOLEUCINE
ASPARTATE
LYSINE
GLUTAMINE
METHIONINE
HISTIDINE
PHENYLALANINE
TYROSINE
J
Serine
Mean Intensity (x10^4 cps)
K
Glycine
Fluorescence Intensity (x10^3)

Figure 3-3 TEPP-46 reduces collagen deposition in fibrotic livers.

(A) Mice were administered with thioacetamide (TAA) at 100mg/Kg for 5 weeks followed by 7 weeks at 250 mg/Kg and TEPP-46 at 50mg/Kg. (B) Livers were collected at the end of 12 weeks and photographed for assessment of surface anatomy. (C) Blood was collected from mice and serum was extracted and aspartate aminotransferase (AST) was measured in the serum using an AST kit. (D) Alanine aminotransferase (ALT) was also measured using an ALT kit. (E) Mice were weighed daily post treatment and recorded to monitor their body weight increases on a weekly basis. (F) Livers were fixed in formalin for 24 hours and embedded in paraffin. They were sectioned at 5µm and were stained for collagen using Sirius red staining kit and were quantified using ImageJ (G) Livers were embedded in OCT and snap frozen in liquid nitrogen and cryosectioned at 5µm. Sectioned were stained for αSMA and observed under a fluorescent microscope and quantified using ImageJ. (H) Cryosectioned livers were stained for PKM2 and observed under a fluorescent microscope and quantified using ImageJ. (I) Livers were powdered under liquid nitrogen and fixed in 50% methanol and deproteinized with chloroform. Free amino acids were analyzed using an Orbitrap LC/MS. (J) Serine levels were analyzed using livers previously prepared and were loaded onto the Orbitral LC/MS system. (K) Glycine levels were analyzed using a kit. Livers were lysed using the provided lysis buffer and the glycine content was measured fluorometrically using a fluorescent microplate reader at Ex/Em 535/587.

3.3.4TEPP-46 reduces fibrosis associated symptoms in the liver

TEPP-46 treated mice showed reduced collagen deposition and fibrosis development in a TAA-ethanol model of liver fibrosis. We observed that the mice gained weight and appeared generally healthier than their vehicle treated counterparts. Therefore, we wanted to explore into the fibrosis associated pathology in the liver. During a fibrotic response, there is an increase in the

inflammatory response which triggers during the early phase of fibrosis. During this time, infiltrating macrophages secrete pro-inflammatory mediators which bring about the activation of the myofibroblasts which further potentiate the fibrotic damage with the secretion of collagen. Resolution of the fibrotic insult in the liver usually results in the amelioration of the inflammatory response. The reduced inflammatory response leads to the reduced activation of the fibroblasts resulting in an inflammation-fibrosis loop. To this end, we hypothesized that the treatment with TEPP-46 lead to the decrease in the inflammatory profile in the liver. We first assessed the percentage of cells which were both αSMA stained with AlexaFluor 555 (Red) and PKM2 positive stained with AlexaFluor 488 (Green) which indicated that the activated myofibroblasts indeed upregulated PKM2 upon activation (Figure 3-4A). PKM2 was observed, although at a lower percentage, in cells which were not αSMA positive. This indicated that the infiltrating macrophages also upregulated PKM2 during the initial pro-inflammatory response. For the initial pro-inflammatory response, the infiltration of macrophages is usually weighted towards M1 phenotype. To assess the infiltration of M1 macrophages we immunostained the cryosectioned livers for CD68, a pro-inflammatory macrophage marker. The levels of CD68 were assessed using immunofluorescence using AlexaFluor 555 (Red) (Figure 3-4B). Levels of CD68 were dramatically decreased upon treatment with TEPP-46 indicating that TEPP-46 reduces the initial macrophage infiltration into the fibrotic liver (Figure 3-4C). The reduction of collagen in the livers observed in the Sirius red stain prompted us to measure the levels of hydroxyproline in the liver lysates. Hydroxyproline is a direct measure of the level of collagen as there is no free hydroxyproline in the cells. The measured hydroxyproline levels were significantly reduced in the TEPP-46 treated mice thereby validating the reduced Sirius red stain intensity observed in the TEPP-46 treated mice (Figure 3-4D). The reduction of the infiltrating macrophages prompted us

to test the levels of pro-inflammatory cytokines IL-1 β, IL-6 and CCL2 in the liver. We also tested the levels of anti-inflammatory cytokines IL-10 to observe if any changes occurred. We extracted mRNA from the livers and cDNA was synthesized. qPCR was performed on the cDNA samples to detect levels of pro-inflammatory cytokines. IL-1 β and IL-6, both pro-inflammatory cytokines, were reduced in the TEPP-46 treated mice consistent with the decrease in the CD68 levels. Surprisingly, the levels of IL-10 increased in the TEPP-46 treated mice which indicates a shift in the inflammatory profile after treatment with TEPP-46. αSMA levels were reduced in the treated mice which was consistent with the reduction in αSMA in the immunofluorescent stain owing to the ROS mediated apoptosis observed in Figure 1.8. (Figure 3-4E).

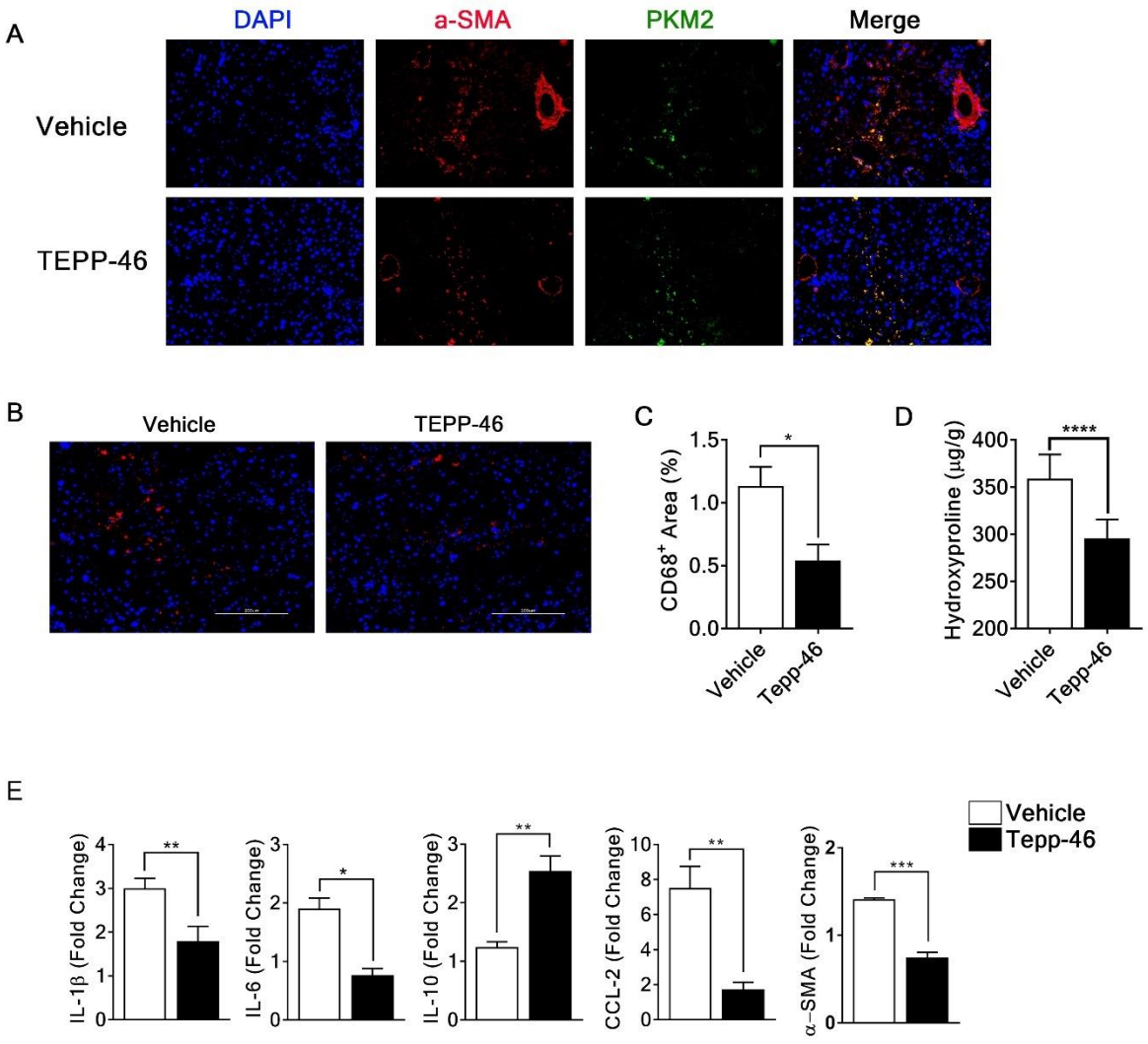

Figure 3-4 TEPP-46 reduces the pro-inflammatory profile in fibrotic livers

(A) Cryosectioned slides were co-stained for αSMA (AlexaFluor 555) and PKM2 (AlexaFluor 488) for the co-localization demonstrating activated myofibroblasts. (B) Cryosectioned slides were subjected to immunofluorescence for CD68 using AlexaFluor 555 for macrophages. (C) Quantification of CD68 positive area in fibrotic livers. (D) Total liver lysates were analyzed for hydroxyproline to assess for collagen levels. (E) RNA from livers was used to synthesize cDNA for the assessment of pro-inflammatory gene expression profile.

3.3.5TEPP-46 reduces lung fibrosis

The effect of PKM2 activator DASA-10 in the acceleration of glycolysis in activated normal lung fibroblasts was observed to be very effective. Therefore, we wondered whether this effect would be translated into an *in vivo* system. To this end, we employed a bleomycin-based lung fibrosis model to evaluate the effect of PKM2 activator TEPP-46 in the amelioration of lung fibrosis. Six-week-old C57BL/6 mice were administered with I.P. bleomycin at 4mg/Kg for 4 weeks. Treatment with TEPP-46 was started at week 4 and was administered for 7 weeks. Mice were euthanized at week 12 and the lungs were collected for further analyses (Figure 3-5A). Mice were euthanized and lungs were assessed for their surface anatomy. TEPP-46 treated mice showed lower surface lesions associated with progression of lung fibrosis (Figure 3-5B). Collected lungs were fixed in formalin for 24 hours and were embedded in paraffin for sectioning. Lungs were sectioned at 5µm and mounted on charged slides for histological analyses. The sectioned tissues were then de-paraffinized and stained for collagen with Masson's trichrome stain. The stain displayed a significantly reduced collagen percentage in the lungs treated with TEPP-46 (Figure 3-5C). The treated lungs show significantly lowered accumulation of collagen fibers in the alveolar sacs and the terminal bronchioles which is a sign of severe lung fibrosis as evidenced by the vehicle treated mice. The slides were analyzed using ImageJ. Since αSMA is one of the markers of myofibroblast activation, we wanted to assess the levels of αSMA in the lungs of the treated mice. Previously cut slides were subject to immunohistochemistry and were probed with an αSMA antibody and were analyzed for stained myofibroblasts (Figure 3-5D). Stained myofibroblasts were observed to be abundant in vehicle treated mice when compared to TEPP-46 treated mice. These data suggest that treatment with TEPP-46 somehow reduces the myofibroblast population in the lungs. This phenomenon is like the αSMA staining observed in the liver. The lungs were then stained for the expression of PKM2 as the expression of PKM2 was associated with the

activation of myofibroblasts in the case of normal lung fibroblasts *in vitro*. Slides were immunostained with a PKM2 antibody. Surprisingly, the levels of PKM2 were not altered in the treated mice which indicates that treatement with TEPP-46 only activates PKM2 and does not alter its expression pattern in the diseased state (Figure 3-5E). To test whether the treatment with TEPP-46 altered the free amino acid profile in lungs, we fixed freshly isolated lungs in 50% methanol and de-proteinized with chloroform. The aqueous layer was then subjected to chromatography using an Orbitrap LC/MS system. The amino acids in the treated group were broadly unaltered apart from proline, valine, isoleucine and glutamine (Figure 3-5F). The altered levels of these seemingly random amino acids were not further investigated. However, we analyzed the levels of serine present in the lung lysates as we did for the liver lysates. Free serine was significantly reduced in the treated lungs when compared to the vehicle lungs (Figure 3-5G). These findings were consistent with the decreased levels of serine in the treated livers. We then proceeded to assess the levels of glycine using a similar method used in the livers. The glycine levels in the treated lungs were significantly reduced when compared to the vehicle lungs (Figure 3-5H). These results confirm our findings that the reduced serine and glycine levels in fibrotic organs leads to the reduced collagen deposition in the organs.

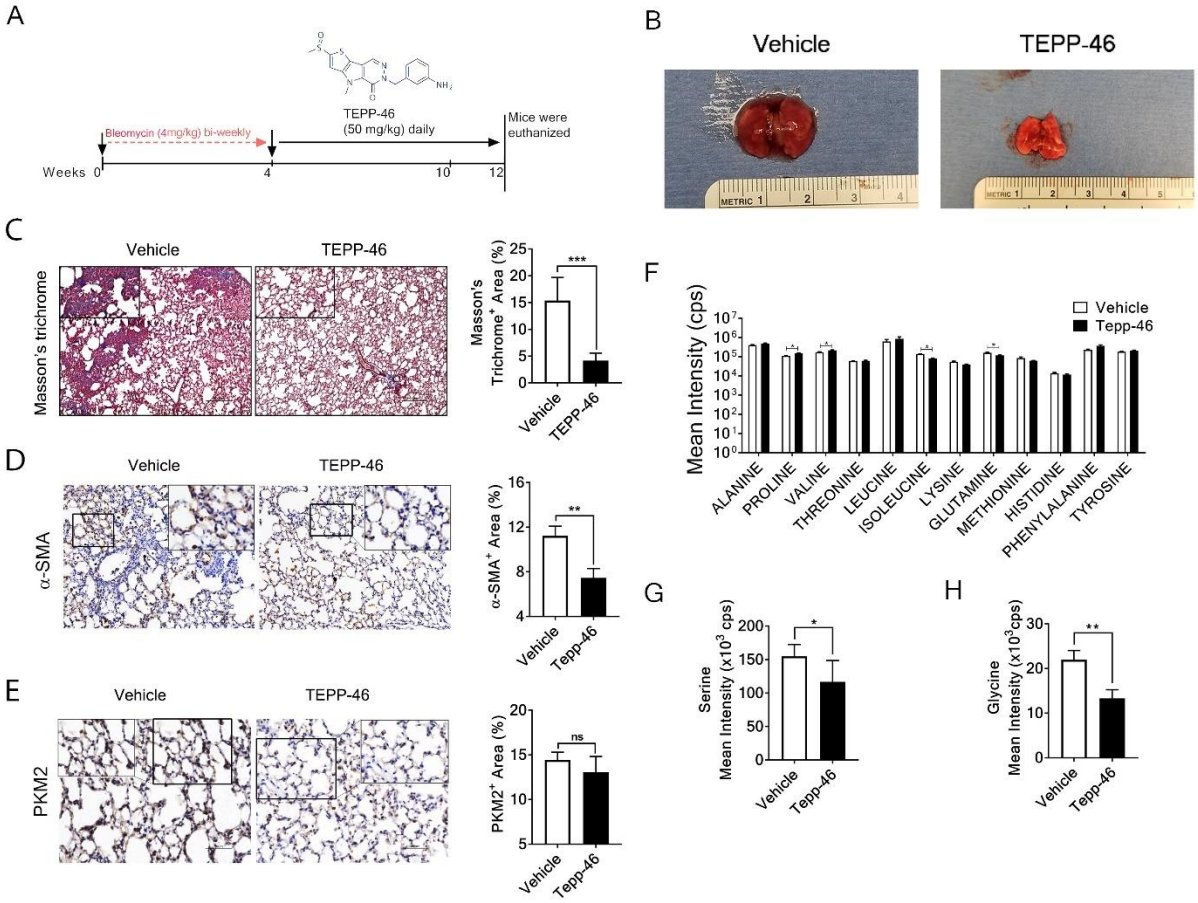
A
TEPP-46
(50 mg/kg) daily
Bleomycin (4mg/kg) bi-weekly
Mice were euthanized
Weeks 0
4
10
12
B
Vehicle
TEPP-46
C
Vehicle
TEPP-46
Masson's trichrome
Masson's Trichrome+ Area (%)
***
Vehicle
TEPP-46
D
Vehicle
TEPP-46
α-SMA
α-SMA+ Area (%)
**
Vehicle
Tepp-46
E
Vehicle
TEPP-46
PKM2
PKM2+ Area (%)
ns
Vehicle
Tepp-46
F
Mean Intensity (cps)
Vehicle
Tepp-46
ALANINE
PROLINE
VALINE
THREONINE
LEUCINE
ISOLEUCINE
LYSINE
GLUTAMINE
METHIONINE
HISTIDINE
PHENYLALANINE
TYROSINE
G
Serine
Mean Intensity (x10³ cps)
*
Vehicle
Tepp-46
H
Glycine
Mean Intensity (x10³cps)
**
Vehicle
Tepp-46

Figure 3-5 TEPP-46 reduces collagen deposition in fibrotic lungs.

(A) Lung fibrosis was induced with bleomycin at 4mg/Kg for 4 weeks. Mice were treated with TEPP-46 for 7 weeks at 50mg/Kg. (B) Lungs were collected photographed for surface anatomy. Vehicle treated mice show surface patches of collagen deposition whereas the TEPP-46 treated lungs showed lower surface aberrations. (C) Formalin fixed paraffin embedded (FFPE) tissues were sectioned and stained for collagen using a Masson's trichrome kit. Cytoplasm is stained in red and collagen is stained in blue. Collagen was quantified using ImageJ. (D) FFPE tissues were subject to immunohistochemistry using a primary antibody towards αSMA and stained with DAB and analyzed using ImageJ. (E) Immunohistochemistry was performed on FFPE tissues with an anti-PKM2 antibody and stained with DAB and analyzed using ImageJ. (F) Lungs were fixed with 50% methanol and free amino acids were extracted with chloroform. Free amino acids were analyzed using an Orbitrap LC/MS system and their mean intensities were measured. (G) Serine was measured using the same Orbitrap LC/MS system and the mean intensity were recorded in both the vehicle and TEPP-46 treated animals. (H) Glycine levels were measured fluorometrically using a glycine kit with the prepared lung lysates. Lysates were measured at Ex/Em 535/587.

3.3.6TEPP-46 reduces fibrosis associated symptoms in lungs

The effect of TEPP-46 in the reduction of serine and glycine levels in total lungs and the subsequent reduction of collagen production by activated myofibroblasts was observed to be significant in the bleomycin model of lung fibrosis. We observed the inflammatory profile was ameliorated in the fibrotic livers when treated with TEPP-46, hence we wanted to test whether a similar phenomenon occurred in the lungs too. To determine the extent of fibrosis in the lungs, their wet weight was recorded. The deposition of collagen in the lungs drastically increased their weight as evidenced in the vehicle treated group. The treatment with TEPP-46 decreased collagen

synthesis and deposition, therefore the weights of the lungs were reduced when compared to the vehicle group (Figure 3-6A). The deposition of collagen was then indirectly measured with the hydroxyproline content present in them. Lungs were lysed with 12N HCl for 24 hours and then measured for hydroxyproline content as hydroxyproline is a specific modification of proline in collagen and there is no free hydroxyproline in the cell. The hydroxyproline content was significantly reduced in the TEPP-46 treated lungs (Figure 3-6B). We then assessed the expression patterns of pro-inflammatory mediators in TEPP-46 treated lungs. We assessed the levels of IL-1□, IL-6. IL-10 and CCL-2. IL-1□ and IL-6 are pro-inflammatory mediators and IL-10 is an anti-inflammatory mediator. CCL-2 is a chemokine known to potentiate macrophage infiltration. αSMA was also measured in the lungs to serve as a control as we have observed the loss of αSMA in both liver and the lungs in the immunohistochemistry stains. IL-1 β and IL-6 have reduced considerably while IL-10 was increased suggesting the inversion of the pro-inflammatory condition in lungs. The expression of CCL2 was also reduced in these lungs which could be the reason of the decreased macrophage infiltration thus leading to decreased pro-inflammatory mediators (Figure 3-6C). The reduction of inflammation in the lungs and the reduction of collagen production and secretion upon treatment with TEPP-46 shows strong resemblance to the treatment profile in the livers. Therefore, the treatment with a PKM2 activator results in the amelioration of fibrosis and its associated symptoms independent of organ which could be used as a potential treatment approach towards fibrosis.

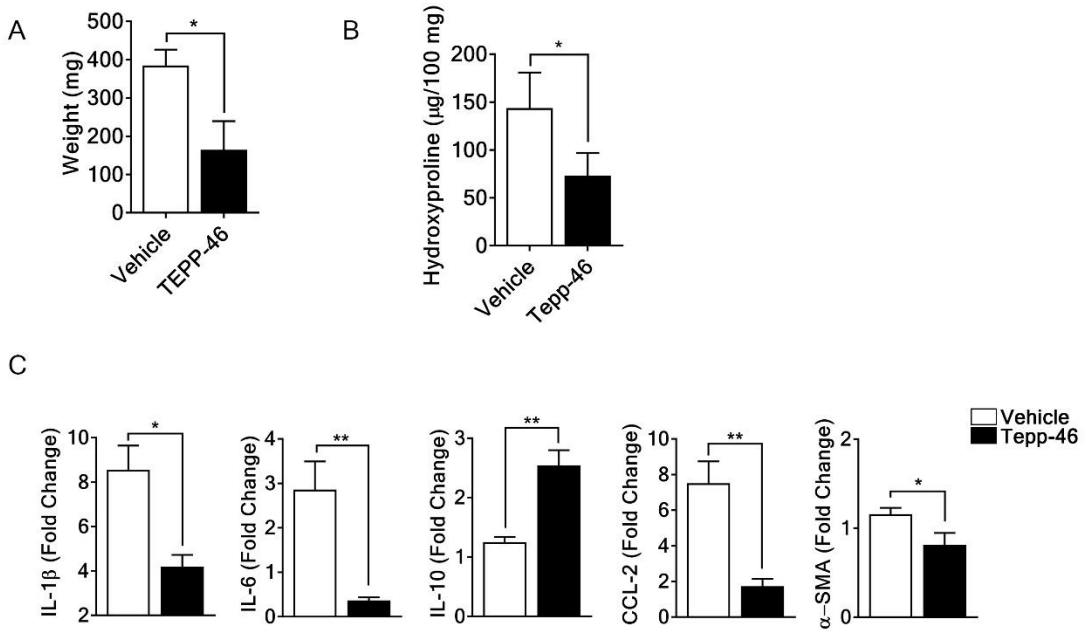

Figure 3-6 TEPP-46 reduces the fibrosis associated symptoms in lungs

(A) Vehicle or TEPP-46 treated mice were euthanized, and wet weights of the lungs were recorded. (B) Vehicle or TEPP-46 treated lungs were lysed in HCl for 24 hours and hydroxyproline content was measured using a kit (Sigma Cat#MAK008). (C) RNA was isolated from treated lungs and 1µg was used for cDNA conversion (Thermo Cat#K1641). RT-PCR was performed for IL1□, IL6, IL-10, CCL2, and αSMA using a SYBR-GREEN system (NEB Cat#M3003L).

3.3.7Alternate splicing of PKM2 is regulated by PTBP1 in activated fibroblasts.

Pyruvate kinase exists in two isoforms namely PKM1 and PKM2. The differences in these isoforms is dependent on the inclusion or the exclusion of exon 10. PKM1 isoform is expressed if exon 9 is included and exon 10 is excluded. PKM2 isoform is expressed if exon 9 is excluded and exon 10 is included. Previous studies in pancreatic cancer cells showed that the alternative splicing of PKM2 is regulated by the expression of heterogeneous nuclear ribonucleoprotein (HNRNP) A1 also known as polypyrimidine tract binding protein 1 (PTBP1). Upregulation of HNRNP A1 leads

to the inclusion of exon 10 in the PKM pre-mRNA and to the production of mature PKM2 mRNA. We observed the upregulation of PKM2 upon TGF-β treatment in both LX2 and NLF cells, which lead us to investigate whether the alternate splicing mechanism of PKM2 was induced in these fibroblasts upon TGF-β mediated activation. To this end, we treated quiescent LX2 and NLF cells with TGF-β to induce the expression of PKM2. We then isolated RNA from these cells and synthesized cDNA to assess the alternate splice profile in activated fibroblasts. We probed cDNA samples with primers specific for exons 9 and 10 within the PKM gene. We used exon 5-6 as a PKM control gene. Upon TGF-β treatment the expression of exon 9 was significantly repressed in both LX2 and NLF cells and simultaneously, exon 10 was significantly upregulated indicating the de-regulation of PKM1 in favor of PKM2. There was no change in the expression of exon 5-6 indicating the change in expression is dependent only in the exon 9-10 interchange (Figure 3-7A). The involvement of PTBP1 in the inclusion of exon 10 was then tested by knocking down PTBP1 with siRNA. LX2 and NLF cells were treated with siPTBP1 for 48 hours and RNA was isolated. 1µg of RNA was converted into cDNA for PCR analysis. Knockdown with siPTBP1 resulted in the repression of exon 10 inclusion resulting in the loss of PKM2 expression. It also increased the inclusion of exon 9 and upregulates the expression of PKM1 (Figure 3-7B). Knockdown of PTBP1 did not however change the inclusion or the exclusion of exon 5 and exon 6 which are common in both PKM1 and PKM2. Therefore, PTBP1 regulates only the inclusion of the splice isoforms of PKM1 and PKM2 but does not change the total expression of the protein. To test whether the inclusion of exon 10 by PTBP1 correlated with the expression of PKM2 protein, we performed a western blot on these cells treated with siPTBP1. We observed the reduction of PKM2 expression in the treated cells. Conversely the treatment with siPTBP1, increased the expression of PKM1 in these cells, which is in line with the RNA levels (Figure 3-7C). We then questioned whether this

switch of metabolic profile from PKM2 to PKM1 upon treatment with siPTBP1 also changed the profile of *de novo* serine and glycine synthesis. We, therefore extracted amino acids from LX2 cells treated with siPTBP1 and subjected them to UV-HPLC to test for the levels of serine and glycine. The levels of serine (Figure 3-7D) and glycine (Figure 3-7E) were significantly reduced in the siPTBP1 treated cells. The involvement of PTBP1 in the inclusion of exon 10 leads to the expression of PKM2 which increases the intermediate buildup which is now relieved with the exclusion of exon 10 and inclusion of exon 9 leading to the expression of PKM1 thereby reducing the buildup of intermediates.

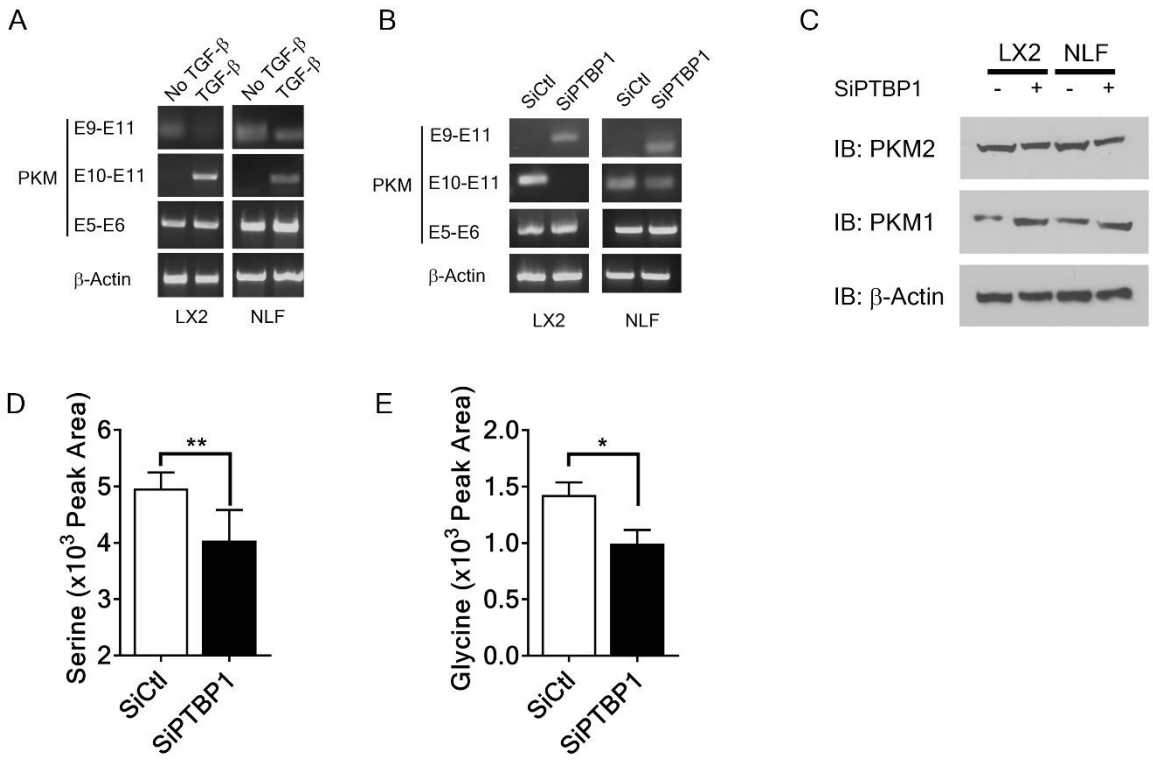

Figure 3-7 PTBP1 regulates the alternate splicing of PKM2 in activated fibroblasts

(A) TGF-β treated LX2 and NLF cells were subject to RNA isolation and cDNA conversion. PCR was performed for exon 9 and exon 10 and for exon 5 and exon 6 and actin as controls. (B) LX2 and NLF cells were treated with siPTBP1 for 48 hours and then were subject to RNA isolation and cDNA conversion. PCR was performed for exon 9 and exon 10 and for exon 5 and exon 6 and actin as controls. (C) siPTBP1 treated LX2 and NLF cells were immunoblotted for PKM1 and PKM2 (D) LX2 cells were treated with siPTBP1 and amino acids were extracted with methanol-chloroform and were analyzed for serine using a UV-HPLC. (E) LX2 treated with siPTBP1 and amino acids were extracted as mentioned above and analyzed for glycine using a UV-HPLC.

3.3.8DASA-10 induces tetramerization of PKM2 in activated fibroblasts

PKM2 is expressed in fibroblasts upon activation with TGF-β and induces Warburg effect in these cells. Warburg effect is characterized by the accumulation of glycolytic intermediates by

reduced pyruvate kinase activity. For pyruvate kinase activity to be lowered, PKM2 is usually in its dimeric state owing to the downstream phosphorylation signaling of TGF-β and the subsequent binding of phosphor-proteins to PKM2. Treatment with DASA-10 mediates the tetramerization of PKM2 by binding to its A-A domains thus potentiating the binding of PEP thereby increasing PKM2 activity. Increased PKM2 activity rapidly depletes the glycolytic intermediates and rescues the cell from its Warburg state thereby restoring normal glycolysis pathway followed by oxidative phosphorylation. Dimer PKM2 is around 150KDa whereas tetramer PKM2 is around 250KDa. To test whether a similar interaction would occur in activated fibroblasts, we treated LX2 cells with 10ng/mL TGF-β for 48 hours and then with 10mM DASA-10 for 24 hours. Cells were lysed in RIPA and proteins were extracted. 2mg of total protein lysate was then subject to FPLC separation using a HiPrep 16/60 Sephacryl S-200 HR column. Separated proteins were eluted in 40 eluates. These eluates were then immunoblotted for PKM2. Activated LX2 cells which were treated with DMSO indicated the presence of PKM2 in eluates #16 to #21 which indicates the dimer form of PKM2. Activated LX2 cells treated with DASA-10 on the other hand indicated the presence of PKM2 in eluates #6-#11 which indicates the tetramer form of PKM2 (Figure 3-8A). Further analysis on the activation of LX2 and NLF cells were performed via immunoblotting for PHGDH (cat no) and collagen-1 (cat no). Upon treatment with TGF-β increased the expression of both PHGDH and collagen-1 (Figure 3-8B). The increase in PHGDH was around 1.5-fold in LX2 cells (Figure 3-8 C left panel) and around 2-fold in NLF cells (Figure 3-8C right panel). The fold change of collagen in LX2 cells was around 3-fold (Figure 3-8D left panel) and around 3.5-fold in NLF cells (Figure 3-8D right panel). We then asked whether the treatment of these activated LX2 and NLF cells with DASA-10 affected the levels of PHGDH. We carried out immunoblots on whole cell lysates for PHGDH and the addition of DASA-10 did not seem to alter the expression levels

of PHGDH in the activated fibroblasts (Figure 3-8E). These results suggest that the reduction of serine observed is due to the lack of the glycolytic intermediate substrate and not due to the reduced enzyme expression.

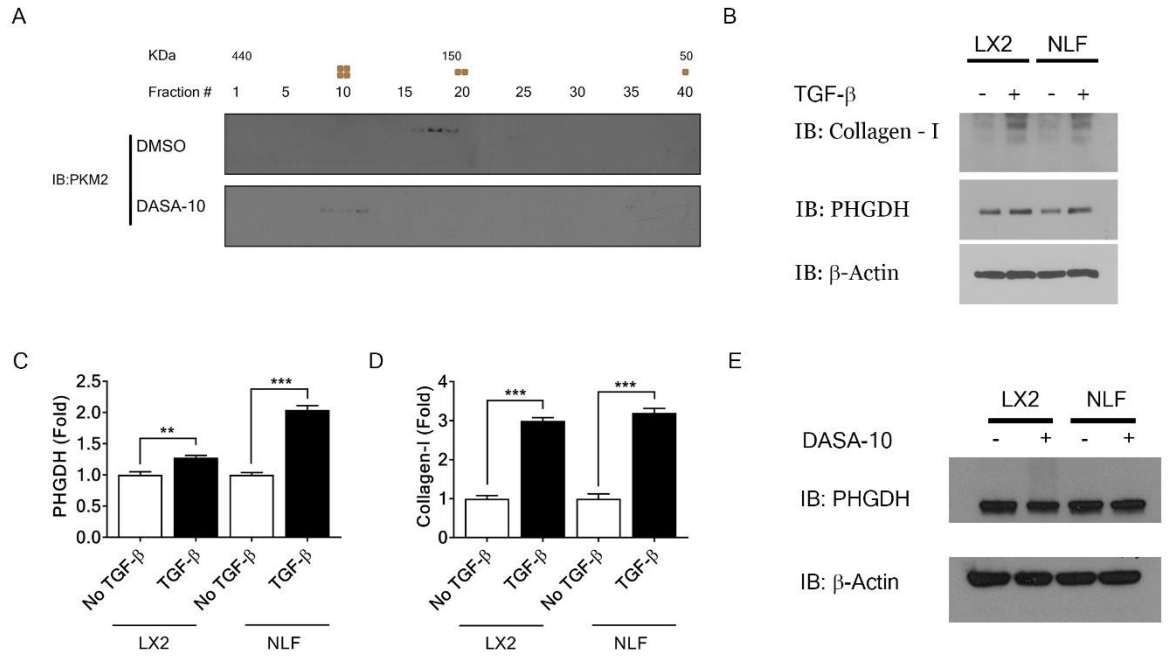

Figure 3-8 DASA-10 promotes tetramerization of activated LX2 cells

(A) LX2 cells were treated with 10ng/mL TGF-β for 48 hours and then treated with either DMSO (top panel) or DASA-10 (bottom panel) and 2mg of total protein was separated using FPLC and immunoblotted for PKM2. (B) LX2 (left panel) and NLF (right panel) cells were treated with 10ng/mL TGF-β for 48 hours and immunoblotted for PHGDH and collagen-1 to verify their activation and collagen secretion profile. (C) Quantification of PHGDH fold increase in band intensity in LX2 (left panel) and NLF (right panel). (D) Quantification of collagen-1 fold increase in band intensity in LX2 (left panel) and NLF (right panel). (E) Activated LX2 and NLF cells were

treated with or without DASA-10 to observer any changes in the protein expression profile of PHGDH.

3.3.9Matrix stiffness regulates glycine synthesis

In the liver, the resident fibroblasts are the hepatic stellate cells. They are quiescent and reside in the space of Disse between the hepatocytes and the sinusoids. The space of Disse in the normal liver is about 5KPa (kilopascals) in pressure. The pressure exerted by the space of Disse however is quite low and is not enough to induce the activation of the hepatic stellate cells, therefore they remain quiescent. Upon fibrotic stimulus, the release of TGF-β from the infiltrating macrophages triggers a massive activation event in the space of Disse. Upon activation, these fibroblasts secrete collagen-1 which increases the matrix pressure exerted in the space of Disse. The quiescent hepatic stellate cells can now respond to the increasing matrix stiffness and can get further activated by mechano-transduction. The fibrotic microenvironment increases the matrix stiffness to around 100KPa which results in hardening of the space of Disse subsequently leading to the hardening of the liver. To test whether the mechano-transduction mediated activation can result in the shift of metabolism towards Warburg effect, we seeded quiescent LX2 cells onto varied pressure regulated plates for 48 hours and then analyzed for levels of glycine. The levels of glycine steadily increased with the increase in simulated matrix stiffness and showed a maximum production of glycine at 100KPa. This was further exaggerated with the addition of TGF-β, thereby further promoting activation and collagen synthesis (Figure 3-9A). We then asked whether the upregulation of glycine under increasing matrix stiffness corresponded with the upregulation of collagen synthesis in these LX2 cells. To that end, we subjected these cells under various pressures to hydroxyproline assay to quantify the production of collagen (Figure 3-9B). The collagen production was indeed upregulated with increasing matrix stiffness thereby providing evidence for

mechano-transduction mediated Warburg effect in activated hepatic stellate cells leading to increased collagen production.

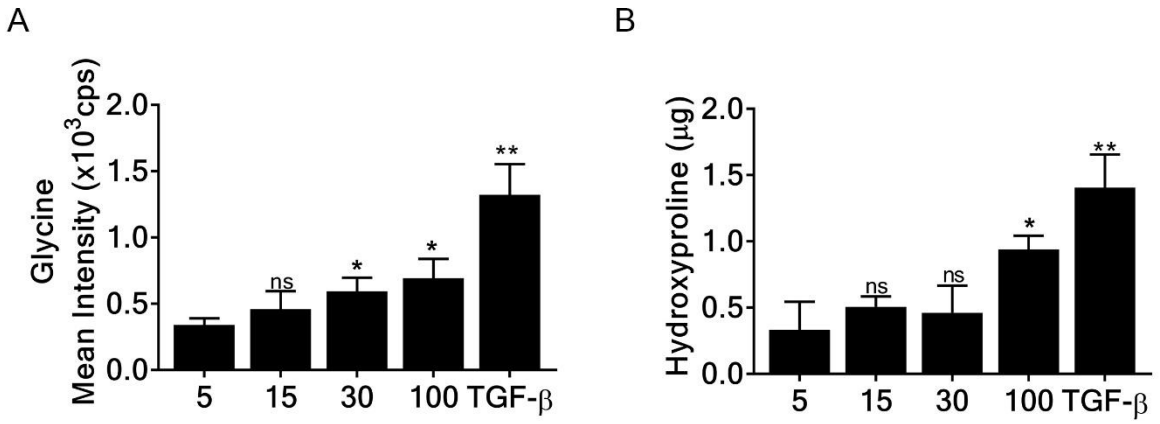

Figure 3-9 Matrix stiffness regulates glycine synthesis

(A) Quiescent LX2 cells were seeded onto differential pressure plates ranging from 5KPa to 100KPa for 48 hours. Cells were then lysed, and amino acids were extracted with methanol-chloroform and glycine levels were analyzed with UV-HPLC. (B) Hydroxyproline levels in LX2 cells seeded on differential pressure plates were measured using a hydroxyproline kit.

3.3.10 DASA-10 induces apoptosis at high concentrations

DASA-10 has been shown to induce apoptosis in lung cancer cells as it rescues cells from Warburg effect. The rescue from Warburg effect depletes the buildup of glycolytic intermediates which are essential for the rapid cell division in cancer cells and the detoxification of ROS by NADPH production. The continued depletion of these vital metabolites in these cancer cells induces apoptosis. We observed the ability of DASA-10 to induce apoptosis under the presence of ROS in activated LX2 cells. We then wanted to test whether DASA-10 alone can induce apoptosis without the presence of ROS stimuli. LX2 and NLF cells were activated with 10ng/mL TGF-β for 48 hours and treated with various concentrations of DASA-10 for 24 hours. Cell viability was

assessed with the MTT assay (Figure 3-10A, 3-10B). In accordance with the previously reported apoptosis in cancer cells, activated LX2 and NLF cells showed decreased cell viability with increasing concentrations of DASA-10. These results indicate an extended role of glycolytic intermediates in the survival and viability of both activated LX2 and NLF cells which lie beyond the *de novo* serine and glycine synthesis.

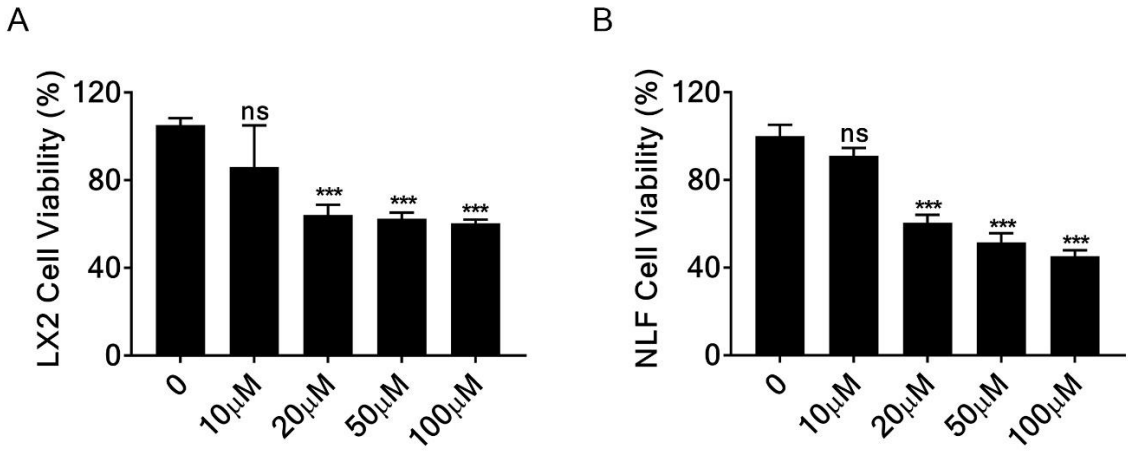

Figure 3-10 DASA-10 induces apoptosis in higher concentrations

(A) LX2 cells were treated with 10ng/mL TGF-β for 48 hours and plated in 96 well plates. They were treated with different concentrations of DASA-10 for 24 hours. MTT assay was performed as per manufacturer's specifications. (B) NLF cells were treated with 10ng/mL TGF-β for 48 hours and plated in 96 well plates. They were treated with different concentrations of DASA-10 for 24 hours. MTT assay was performed as per manufacturer's specifications.

3.3.11 DASA-10 alters the enzymes of the serine pathway

The *de novo* synthesis of serine requires the accumulation of the glycolytic intermediate, 3-phosphoglycerate (3-PG). 3-PG is the initial substrate that leads into a series of reactions towards the synthesis of serine. In physiological glycolysis, 3-PG is readily converted into 2-PG by

phosphoglycero-mutase. During the advent of Warburg effect, the upregulation of PKM2 leads to reduced glycolytic output and increased accumulation of the intermediates. Along with the upregulation of PKM2, the activation of fibroblasts leads to the upregulation of 3-phosphoglycerate dehydrogenase (PHGDH) which facilitates the initial step of the oxidation of 3-phosphoglycerate into 3-phosphopyruvate. This reaction is irreversible and commits 3-PG towards serine synthesis. 3-phosphopyruvate is then converted into 3-phosphoserine by phosphoserine aminotransferase (PSAT1). 3-Phosphoserine is then converted into serine by removal of the phosphate group by phosphoserine phosphatase (PSPH). Serine can then be readily interconverted into glycine by serine hydroxymethyl transferase (SHMT1/2). We observed the upregulation of PHGDH in the activated fibroblasts, and we then asked whether the activation affected the status of the downstream enzymes in the serine synthesis pathway. We checked the expression profiles of all the above-mentioned intermediate enzymes using qPCR from both DMSO and DASA-10 treated activated LX2 cells (figure 3-11A). We also checked the expression profiles of COL1A1 and PKM2 in the LX2 and NLF cells treated with DMSO or DASA. The DMSO treated cells showed a significant increase in the expression of these enzymes as evidenced in the DMSO treated cells. However, the addition of DASA-10 resulted in no apparent change in the expression profile of both COL1A1 and PKM2. This indicates that the resulting reduction in the collagen production is not transcriptionally controlled but metabolically regulated. This, however, ceases to be the case in the expression profiles of the enzymes of serine synthesis. DASA-10 appears to have reduced the levels of PHGDH, PSAT1, SHMT1, SHMT2 but not PSPH. These results collectively indicate that the regulation of serine by DASA-10 is controlled by another mechanism independent of glycolytic activation by biding to PKM2. We, however, have not explored the reasoning behind the reduction of these enzymes upon treatment with DASA-10.

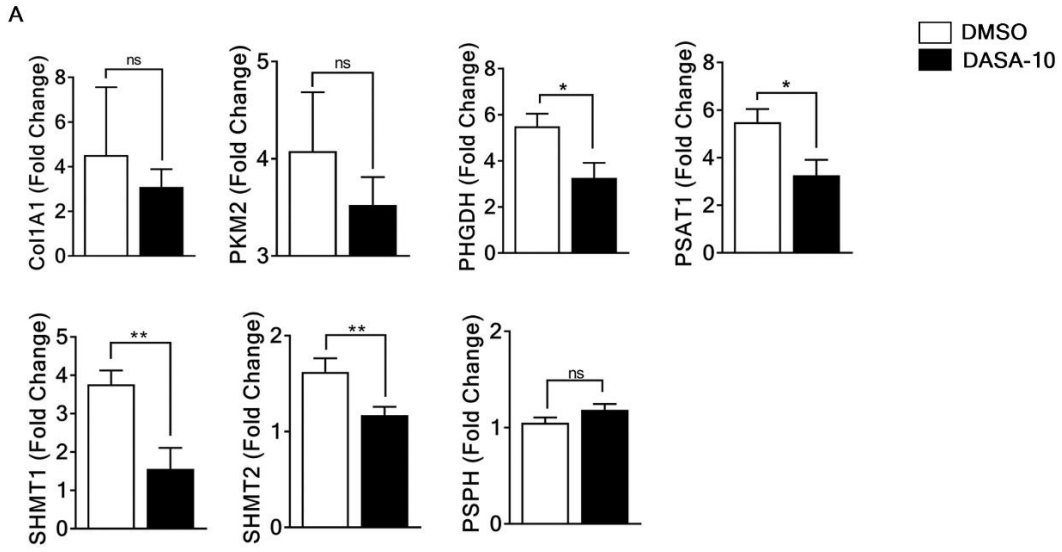

Figure 3-11 DASA-10 regulates the levels of serine synthesis enzymes

(A) qPCR was performed on activated LX2 cells treated with either DMSO or DASA-10 and enzymes of the serine synthesis pathway were quantified along with COL1A1 and PKM2.

4 PYRUVATE KINASE IN LOX REGULATION

4.1 Abstract

Hypoxia activates Hif-1α which induces expression of a variety of genes, including lysyl oxidase (LOX). LOX is a secreted copper dependent amine oxidase, oxidizing lysine residues in its substrate proteins. Oxidization of lysine in collagen leads to crosslinking of this important extracellular matrix protein, consequentially resulting in collagen bundles which leads to the progression of organ/tissue fibrosis. PKM2 mediates Hif-1α activity in cells under hypoxic conditions. Here, we report that the PKM2- Hif-1α axis induces LOX expression in fibroblasts and cancer cells. PKM2-Hif-1α complex regulates LOX transcription by directly binding to LOX promoter. Our experiments show reduction in both LOX mRNA in fibroblasts and cancer cells and secretion by the cells upon PKM2 knockdown and treatment with PKM2 activators. Consequently,

PKM2 activators reduce crosslinked collagen in tumors, fibrotic livers and lungs, which ameliorates tumor metastasis and hepatic and lung fibrosis. Our study suggests that PKM2-Hif-1□ axis is required for LOX expression and secretion in multiple pathological conditions. Our results indicate that pyruvate kinase inactive dimer mediates Hif-1α in regulating LOX. Evidently, our study uncovers an important common targetable pathway for treatment of pathological fibrosis.

4.2 Introduction

Hypoxia is a physiological phenomenon where there is lack of the availability of oxygen. When there is a dearth of oxygen in the tissue, it triggers a cascade of events leading to the upregulation a plethora of genes some of which help in the restoration of oxygen supply to the hypoxic region. In normoxic environments, hypoxia inducible factor-1α (HIF-1α) is hydroxylated by prolyl hydroxylase (PHD) by using O_2 as a substrate. Lysine hydroxylated HIF-1α can now bind to the von Hippel-Lindau tumor suppressor protein (VHL). The association between HIF-1α and VHL leads to the poly-ubiquitination of HIF-1α leading to its proteosomal degradation. Under hypoxic conditions, the lack of O_2 removes the ability of PHD to hydroxylate the lysine residues on HIF-1α. Without the hydroxylated lysines, VHL cannot bind to HIF-1α and its consequently protected from ubiquitin mediated degradation. Stabilized HIF-1α can freely enter the nucleus to promote gene transcription.

Pyruvate kinase is a glycolytic enzyme involved in the final step of glycolysis. Pyruvate kinase is expressed in multiple isoforms, M1, M2, R and L. PKM1 and PKM2 are splice isoforms regulated by PTBP1 by the inclusion of exon 9 yielding PKM1 or inclusion of exon 10 yielding exon 10. PKR is the isoform present in erythrocytes. PKL is the isoform present in hepatocytes. PKM1 is ubiquitously expressed in all tissues whereas PKM2 is expressed in embryonic and proliferative tissues. PKM2 has been implicated in multiple cancers wherein

expression of PKM2 is correlated with lower overall survival and lower progression free survival. Several studies indicate that the expression of PKM2 promotes cancer cell survival and metastasis. PKM2 exists in two states, dimer form or tetramer form. The dimer form of PKM2 has a low glycolytic activity and leads to increased glycolytic accumulation and improves anabolic processes whereas tetrameric PKM2 has high glycolytic activity and leads to depletion of glycolytic intermediates. The non-metabolic role of PKM2 has also been widely studied wherein dimer PKM2 can act as a protein kinase. Dimer PKM2 is shown to associate with HIF-1α in macrophages to localize to the nucleus to upregulate IL-1β. In activated fibroblasts, PKM2 is upregulated and exists in dimer form and induces Warburg effect to promote survivability and collagen synthesis. We thereby tested the effects of dimer PKM2 and its association with HIF-1α in activated fibroblasts and its relevance in progression of fibrotic diseases. We also tested the effect of tetramerization of PKM2 in the association with HIF-1α and its effectiveness in the amelioration of fibrosis.

4.3 Results

4.3.1 Hypoxia upregulates LOX in activated fibroblasts

Hypoxia is a hallmark characteristic of many tumors. The core of the tumor is usually necrotic due to the massive cell death that usually occurs due to the core inflammation provided by the infiltrating neutrophils, macrophages and T-cells. The tumor core is usually not extensively vascularized leading to a lowered O_2 tension. Lowered oxygen is sensed by the tumor cells and the microenvironment and in response to low oxygen, these cells induce the stabilization of Hif-1α. Hif-1α is translocated into the nucleus and binds to a stretch of DNA called the hypoxia response element (HRE). Binding of Hif-1α to the HRE aids in the transcription of HRE genes. Hypoxia can regulate a myriad of genes and the most significant of those is VEGF which induces neo-vascularization in the tumor. This enables the tumor to facilitate increased oxygen and nutrient

delivery. Lysyl oxidase family proteins namely lysyl oxidase (LOX) and lysyl oxidase like 2 protein (LOXL2) also respond to the upregulated hypoxia and transcription of these genes are facilitated. Similarly, the microenvironment in a fibrotic tissue is hypoxic owing to the accumulation of ECM in the space of Disse in the liver and the alveolar sacs in the lungs. In both these organs, upon fibrotic insult, these spaces tend to fill-up with fibrillar type I and type III collagens which leads to the inability to freely diffuse metabolites especially molecular O_2. This leads to lowered O2 tension in these tissues and stabilization of HIF-1α and subsequent activation of HRE elements and upregulation of HRE genes. To test whether hypoxia can induce the expression of LOX and LOXL2, we cultured LX2 cells in 1% saturated O_2 for 6, 12 and 24 hours. These cells were then lysed and immunoblotted for LOX (Fig 4.1A). LOX was indeed upregulated upon induction with 1% O_2 condition for 6 hours and steadily increased with longer incubation (Figure 4.1B). We then tested whether the upregulation of hypoxia directly induced LOX and LOXL2 mRNA expression in these cells. We incubated LX2 cells for in 1% O_2 24 hours and analyzed LOX (Figure 4.1C) and LOXL2 (Figure 4.1D) expression via qPCR. Both LOX and LOXL2 were significantly upregulated in the cells exposed to hypoxia when compared to the cells under normoxia. Therefore, hypoxia directly upregulated the expression of both LOX and LOXL2 in cancer cells.

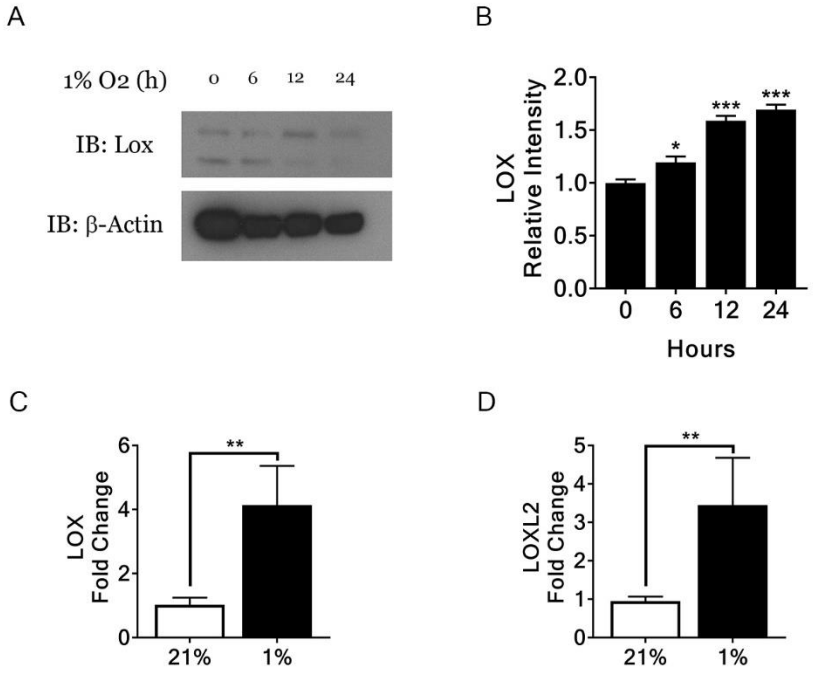

Figure 4-1 Hypoxia directly upregulates LOX and LOXL2 in LX2 cells

(A) $1x10^6$ LX2 cells were incubated in a hypoxia chamber and flushed with 1% O_2 for 24 hours and 30µg was immunoblotted for the presence of LOX. (B) LOX band intensities were measured using ImageJ and compared to normoxia conditions. (C) mRNA was isolated from $1x10^6$ LX2 cells and converted into cDNA. qPCR was performed to analyze LOX expression under hypoxia. (D) Previously converted cDNA was used for qPCR for LOXL2 expression under hypoxia.

4.3.2DASA-10 Reduces LOX expression in fibroblasts

The role of PKM2 was tested in the expression of hypoxia response element genes. Under hypoxic conditions, PKM2 is known to associate with Hif-1α and translocate into the nucleus. We hypothesized that the reason for PKM2 to bind to Hif-1α was the dimer conformation of PKM2 as the tetramer conformation of PKM2 is bound to the glycolytic complex. To this end, we tested the effects of PKM2 activator, DASA-10 on Hif-1α's ability to induce the expression of LOX and

LOXL2 in cells grown in hypoxia. We treated LX2 cells and NLF cells with 10μM DASA-10 and then incubated them in a hypoxia chamber flushed with 1% O_2 for 24 hours. We subjected the cells to immunoblots for LOX. Treatment with DASA-10 significantly reduced the levels of LOX protein in these cells (Figure 4.2A). Relative band intensities were quantified with ImageJ to quantify the fold change decrease of LOX production in DASA-10 treated cells (Figure 4.2B). We then wondered whether the treatment with DASA-10 resulted in the reduced transcriptional regulation provided by Hif-1α. To test this hypothesis, we treated LX2 and NLF cells with 10μM DASA-10 and were incubated in a hypoxia chamber as before and mRNA was isolated. 2μg of RNA was then converted to cDNA and qPCR was performed to test the expression levels of LOX and LOXL2. The expression profile of both LOX and LOXL2 in LX2 cells (Figure 4.2C) and NLF cells (Figure 4.2D) was reduced significantly post treatment with DASA-10 indicating that DASA-10 mediated tetramerization of PKM2 reduced the ability of Hif-1α to upregulate both LOX and LOXL2. This indicates that PKM2's binding to Hif-1α acts as a transcription enhancer and this effect is reduced upon tetramerization with DASA-10.

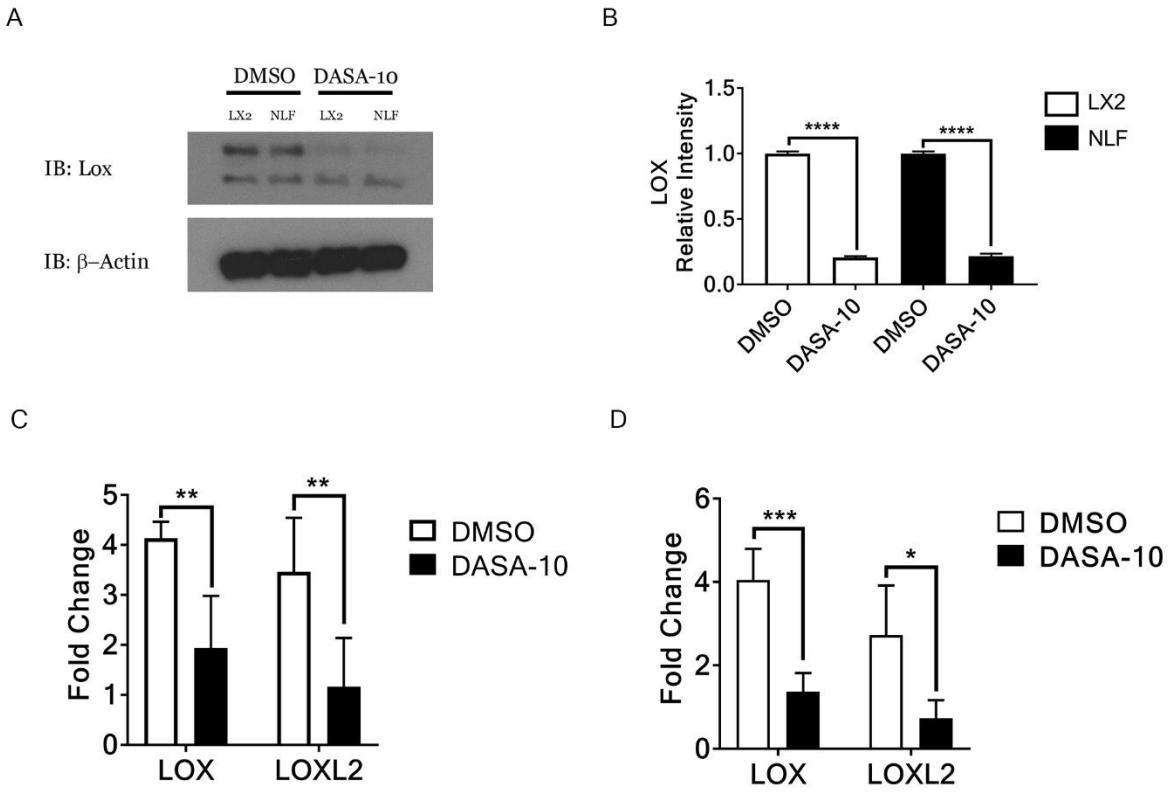

Figure 4-2 DASA-10 reduces LOX and LOXL2 expression

(A) $1x10^6$ LX2 and NLF cells were treated with either DMSO or 10μM DASA-10 and cultured under hypoxia for 24 hours. (B) Relative band intensities were calculated for both LOX and LOXL2 using ImageJ. (C) mRNA was isolated and converted into cDNA and qPCR was performed for the expression of LOX and LOXL2 in LX2 cells. (D) mRNA was isolated and converted into cDNA and qPCR was performed for the expression of LOX and LOXL2 in NLF cells.

4.3.3DASA-10 reduces nuclear localization of PKM2

For PKM2 to regulate Hif-1α's transcriptional capability, it could potentially physically associate with Hif-1α under hypoxia and translocate into the nucleus as a complex. Treatment of these cells with DASA-10 abrogates this association due to the tetramerization of PKM2 and

confining it into the glycolytic complex. To test this, we cultured LX2 cells in hypoxia and treated them with either DMSO or 10μM DASA-10 for 24 hours. We then performed immunofluorescence for both PKM2 and Hif-1α to observe whether there was any detectable co-localization in the nucleus or in the cytoplasm. Evidently, hypoxia induced the association of PKM2 with Hif-1α was visible in the DMSO treated cells in the nucleus. Hif-1α, stained green, PKM2, stained red and the nuclear counterstain, DAPI, stained blue, were all co-localized in the nucleus leading to the overlapped white spots indicating the presence of all three proteins. In the DASA-10 treated cells, the intensity of the co-localization was reduced as evidenced by the reduced presence of the overlapping white spots. These results indicate that under hypoxic conditions, PKM2 associates with Hif-1α and translocates into the nucleus and this association is disrupted by the treatment with DASA-10 (Figure 4-3).

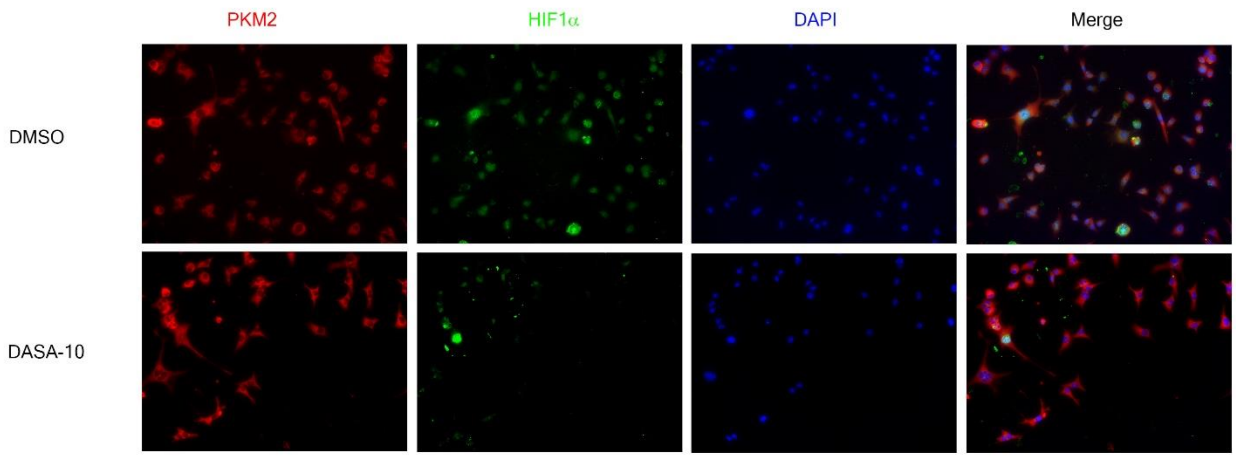

Figure 4-3 DASA-10 reduces nuclear localization of PKM2 and Hif-1α

(A) LX2 cells were seeded onto glass slides and were treated with either DMSO or 10μM DASA-10 and cultured under hypoxia for 24 hours. PKM2 was probed with Alexa-Fluor 555 conjugated antibody and Hif-1α was probed with Alexa-Fluor 488 conjugated antibody and counterstained with DAPI and co-localization was assessed in the nucleus. (B) Co-localization was analyzed using the Pearson method and quantified using ImageJ.

4.3.4TEPP-46 reduces LOX in models of fibrosis

In models of liver and lung fibrosis, several LOX family proteins are secreted by the activated resident fibroblasts which help in the crosslinking of ECM proteins mainly collagens and elastins. In the fibrotic microenvironment, there is lowered O_2 tension leading to the stabilization of Hif-1α and that leads to the expression of LOX and its family proteins. In both liver and lung models of fibrosis, fibrotic stimulus stimulates the resident fibroblasts to secrete ECM and subsequently secrete LOX and its family proteins. Therefore, we tested the effects of a PKM2 activator, TEPP-46 in the production of LOX in liver and lung fibrosis models. Liver fibrosis was induced with the TAA-ethanol model for 12 weeks and then were treated with 50mg/Kg TEPP-46 for 35 days. Lung fibrosis was induced with the bleomycin model for 4 weeks. Mice were treated

with 50mg/Kg TEPP-46 for 35 days. Respective organs were harvested and fixed in 4% paraformaldehyde and embedded in paraffin. 5µm sections were mounted onto slides and IHC was performed for LOX in both liver and lung tissues. Treatment with TEPP-46 resulted in significant reduction in LOX expression level in the lungs (Figure 4.4A top panel) and in the liver (Figure 4.4A bottom panel). LOX levels were especially reduced in the alveolar spaces in the lungs and in the liver parenchyma indicating that TEPP-46 effectively blocked the transcription of LOX by interrupting the binding between PKM2 and Hif-1α in these fibrotic tissues. LOX stained area was quantified using ImageJ in both lung and liver tissues (Figure 4.4B). We then questioned whether the reduction in the expression of LOX in these tissues resulted in the decrease in the activity of LOX in the tissue and in the serum. To this end we tested LOX activity in whole lung lysate and from serum obtained from treated mice (Figure 4.4C). Evidently, the treatment with TEPP-46 resulted in decreased LOX activity in both the lung lysates and the serum. We also tested the LOX activity in total liver lysates and in the serum from the treated animals. Like the LOX activity in the lungs, LOX activity was reduced significantly in both the liver lysates and in the serum of these animals. These results suggest that the treatment with TEPP-46 reduces the expression of total LOX in the fibrotic organs and further reduces its activity in the tissue as well as the serum leading to lowered collagen crosslinking and reduced tissue damage and restores tissue function.

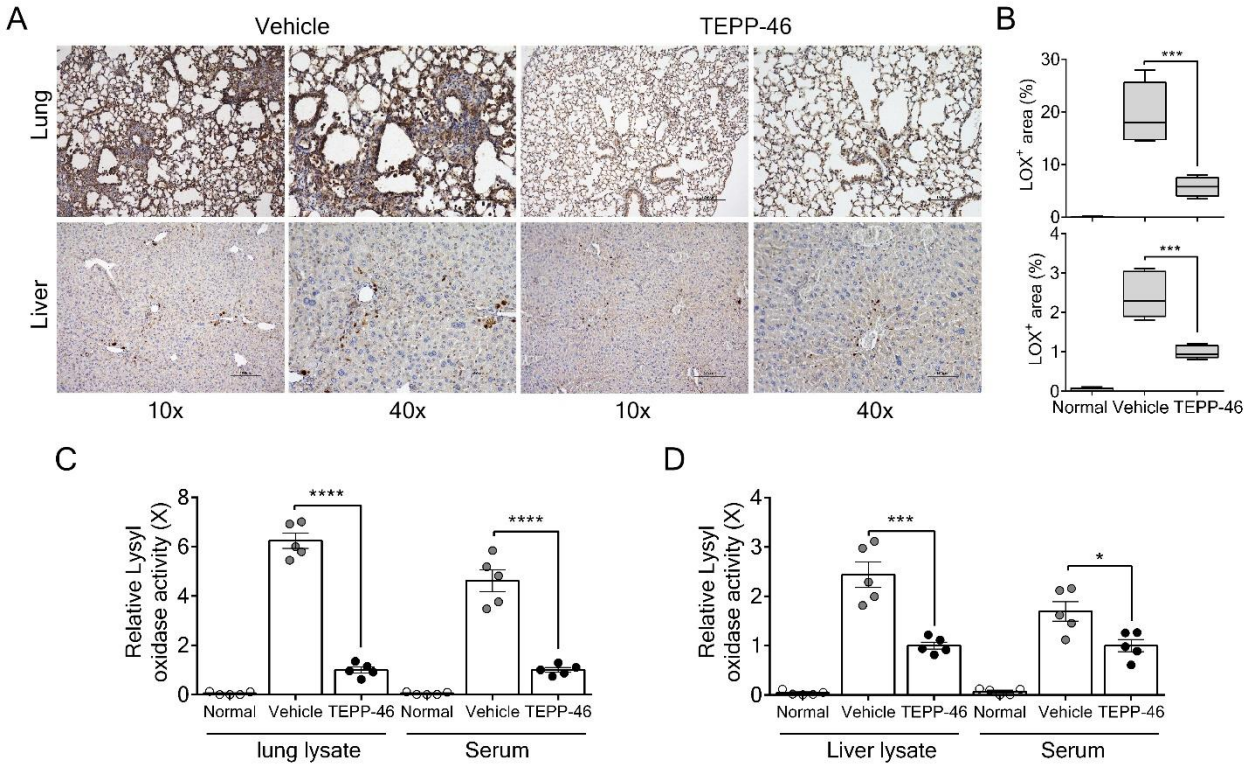

Figure 4-4 TEPP-46 reduces LOX expression *in vivo*

(A) FFPE lungs (top panel) and liver (bottom panel) were sectioned at 5µm and probed for LOX via immunohistochemistry. (B) LOX positive area was quantified using ImageJ in both lungs (top panel) and liver (bottom panel). (C) LOX activity assay was measured using a LOX activity kit (cat no) in bot lung lysates (left columns) and serum (right columns) in bleomycin model of lung fibrosis. (D) LOX activity assay was measured using a LOX activity kit in bot lung lysates (left columns) and serum (right columns) in bleomycin model of lung fibrosis.

5 Conclusions and Discussion

5.1 Altered metabolism in activated fibroblasts

Quiescent fibroblasts residing in the tissue during homeostasis are not metabolically active and do not have increased demand for fuel to perform their functions. In this state, the cell uses glucose

to generate ATP via citric acid cycle. Glucose is utilized in an energy efficient manner in quiescent fibroblasts wherein the glycolytic intermediates are shuttled down the glycolytic pathway towards pyruvate production. The produced pyruvate is then converted into Acetyl CoA which is then shunted into the citric acid cycle and further down into the electron transport chain for the synthesis of ATP. The normal production of ATP is sufficient for the quiescent fibroblasts for their functions. Conversely, activated fibroblasts differ in their energy requirements. Activated fibroblasts have an increased rate of transcription and subsequently increased rate of translation. Accompanying the increased transcription and translation, activated fibroblasts have increased secretion profile wherein they secrete the major ECM proteins including collagen, elastin, laminin and fibronectin. All of these processes require massive energy production. To keep up with the differentiated state of the fibroblasts, the cell undergoes a myriad of changes which aid in the increased energy demands of the cell. Activated fibroblasts upregulate pyruvate kinase M2 which initiates a metabolic switch. In this event, PKM2 does not however, efficiently convert phosphoenolpyruvate (PEP) into pyruvate. This is due to the dimeric state of PKM2 which makes it less efficient in the production of pyruvate. The lowered glycolytic index leads to the accumulation of the glycolytic intermediates. The glycolytic intermediates have a multitude of functions in the cell. Starting with glucose-6-phosphate which can be shunted into the pentose phosphate pathway which leads to the production of ribose-5-phosphate which is then used for the incorporation of DNA during replication. Another important glycolytic intermediate is 3-phosphoglycerate which is used in the *de novo* serine synthesis. The inability of dimeric PKM2 to synthesize pyruvate reduces the production of Acetyl-CoA therefore reduces the citric acid cycle output and reduces efficient ATP synthesis. The switch towards this inefficient energy synthesis is termed ‘Warburg effect’. This phenomenon is usually observed in cancer cells which use this

inefficient energy production system but still remain viable due to the presence of the glycolytic intermediate fueled anabolic processes. We observed that the metabolic switch in activated fibroblasts is like that of in cancer cells wherein the activated fibroblasts fuel their need for protein synthesis and secretion by switching to anabolic processes.

5.2 Dimer PKM2 drives de novo collagen synthesis

PKM2 can exist in two states based on the cellular signals present in the cell. The dimeric form of PKM2 has low glycolytic efficiency whereas its tetrameric form has high glycolytic activity. The two multimeric states of PKM2 can be interchanged by the binding of several molecules ranging from endogenous glycolytic intermediate like fructose-1,6-bis-phosphate (F-1,6-BP) to synthetically designed DASA/TEPP family of PKM2 activators. The dimeric form of PKM2 present in the myofibroblasts enables the accumulation of glycolytic intermediates. 2-phosphoglycerate (2PG) is one such glycolytic intermediate which can be shunted into the *de novo* serine synthesis pathway by the enzyme phosphoglycerate dehydrogenase (PHGDH). Synthesized serine is readily converted into glycine by the action of serine hydroxmethyl transferase (SHMT1/2). Glycine is an important amino acid in the assembly of collagen fibrils wherein every third residue is glycine in an XaaYaaGly formation. The accumulated glycolytic intermediates provide substrate for the action of PHGDH and subsequently for the synthesis of serine and glycine. This flux of metabolites into collagen synthesis is possible only due to the lowered glycolytic index of dimeric PKM2. Thereby, in an activated myofibroblasts, the significance of PKM2 expression and its conversion into its dimeric form is essential for the cells to be able to readily synthesize collagen.

5.3 PKM2 activators reduce anabolic processes

The dimeric PKM2 is an essential requirement for meeting the energy needs of a metabolically active cell. In a proliferating cell, the incoming growth factor signal triggers a cascade of

intracellular protein phosphorylation for downstream signaling. PKM2 can bind to tyrosine phosphorylated proteins and be converted into its dimeric state. This stops the flux of pyruvate into the citric acid cycle thereby upregulating glycolytic intermediates. The intermediates of glycolysis can be used for the biosynthesis of several crucial molecules required by the cell for proliferation and survival. The pentose phosphate pathway (PPP) is an essential anabolic pathway mediated by glucose-6-phosphate dehydrogenase which readily oxidizes glucose-6-phosphate and shunts it towards the synthesis of ribose-5-phosphate which is an essential nucleotide for DNA synthesis. The ribose-5-phosphate synthesized from PPP is rapidly used by a cell for its proliferative needs. The *de novo* synthesis of serine from 2PG is upregulated in several cancer cells as well as activated fibroblasts. Serine is an important resource in the cell as it donates a carbon atom towards the one-carbon metabolism in the cell. The one-carbon metabolism is responsible for the methylation of several proteins including histones and the methylation of DNA and RNA. Methylated histones and DNA aid in the unraveling of the chromosome to aid in the transcription of genes. The presence of endogenous or an exogenous PKM2 activator molecules bind to dimeric PKM2 and potentiate the formation of tetrameric PKM2. The DASA/TEPP family of synthetic activators can bind to PKM2 away from the F-1,6-BP binding site and can retain PKM2 in its tetrameric state even under growth factor signaling. The presence of these strong activators leads to the persistent activation of PKM2 thereby rapidly depleting the anabolic processes mentioned. Therefore, the activity of PKM2 directly affects the fate of R5P and the one-carbon metabolism in the cell thereby disrupting its optimal proliferative and metabolic activities.

5.4 Tetrameric PKM2 aids in ROS induced apoptosis

The ability of a cell to resist the reactive oxygen species produced during phases of oxidative stress is dependent upon several electron donor species present in the cell which can readily

convert the ROS into water and can interconvert into their oxidized form. The major molecule to combat the presence of ROS in a cell is its reduced glutathione (GSH) stores. GSH can be freely oxidized to oxidized glutathione (GSSG). The dynamic balance within the cell to efficiently utilize GSH to reduce ROS is dependent on the rapid conversion of GSSG back into GSH to further potentiate the reduction of ROS. The conversion of GSSG to GSH is dependent on NADPH. NADPH provides the reducing power for the cell by maintaining the GSH/GSSH ratio. The major source of NADPH is indeed the PPP wherein the reduction $NADP^+$ is potentiated by glucose-6-phosphate dehydrogenase and 6-phosphogluconate dehydrogenase. The dimeric form of PKM2 upregulates the PPP and maintains the production of NADPH and thus the reducing power of the cell. Tetramerization of PKM2 decreases the flux of G6P into the PPP thereby reducing the NADPH generated in the cell. Therefore, in cells treated with DASA/TEPP family activators, there a decreased level of NADPH and this leads to a lower reducing power in the cell. These cells now lack protection against ROS and therefore undergo apoptosis. The activity of PKM2 is responsible for the protection of the cell against ROS mediated apoptosis.

5.5 PKM2 and the fibrotic process

In the fibroblast, the process of collagen synthesis and secretion is initiated by TGF-β. The activation of fibroblasts upregulates a plethora of genes which aid in the proliferation of the fibroblast and in the secretion of ECM. PKM2, PHGDH, COL1A1, αSMA are some of the few genes dependent on TGF-β. PKM2 leads to the increased glycolytic flux into the several anabolic processes including the *de novo* serine synthesis owing to the upregulation of PHGDH. Synthesized serine and subsequently glycine, aid in the assembly of collagen fibrils. Secretion of assembled collagen is one of the hallmark characteristics of the development of fibrosis. Fibrosis of the liver, lung and other organs, leads to the structural and functional decline eventually to organ

failure. The interplay between the expression of PKM2 and the secretion of collagen leads to the steady disease state. The progression of disease is directly correlated with the expression of PKM2 and its lowered activity. The metabolic flux of the glycolytic intermediates into the serine/glycine synthesis maintains the constant supply necessary for the pathological secretion of collagen. Therapeutic intervention with PKM2 activators leads to the reduction in the levels of glycine and lowers the production of collagen. This dampens the progression of fibrosis in the organ and reduces the morbidity and mortality due to fibrotic insult.

5.6 PKM2 regulates hypoxia response elements

Hypoxic environments reduce available molecular oxygen. Lowered O_2 tension in the cell leads to the stabilization of HIF-1α by reducing the activity of prolyl hydroxylase (PHD) and the binding of von Hippel-Lindau tumor suppressor protein (VHL) thereby reducing the ubiquitination of HIF-1α. Stabilized HIF-1α is now accessible for free nuclear localization and downstream gene transcription. The upregulation of hypoxia is usually observed in poorly vascularized tumors which have low levels of molecular oxygen available for the tumor load. It has been recently observed that in cancer cells, HIF-1α translocation into the nucleus is aided by the binding of PKM2 to it. In cancer cells, PKM2 and HIF-1α are both available in abundance and therefore the PKM2-HIF-1α complex efficiently translocates into the nucleus and upregulates hypoxia response elements (HREs). Interrupting this association lead to reduced HIF-1α nuclear localization and lowered expression of HRE genes. In activated fibroblasts, PKM2 is upregulated for the induction of Warburg effect and for the survival of the cell. Activated fibroblasts secrete collagen which can interfere with the free blood flow through the organ thereby reducing the O_2 tension in the fibrotic area. This phenomenon stabilizes HIF-1α and promotes its nuclear localization. We observed the PKM2-HIF-1α association in activated

fibroblasts for the first time. This association increased the expression of HRE genes like in cancer cells. Activated fibroblasts secrete lysyl oxidase (LOX) to enable collagen crosslinking in the extracellular space. The treatment of these activated fibroblasts with PKM2 activators abrogated the association with HIF-1α by inducing tetramerization of PKM2 and reduced the expression and secretion of LOX by the fibroblasts. Therefore, PKM2 activators are a potential therapeutic avenue for tackling collagen crosslinking in fibrotic diseases.

5.7 Final Conclusions

We have tested the effects of PKM2 in the activation of fibroblasts and their impact on fibroblast metabolism. We have, for the first time, showed that the activation of PKM2 induces the tetramerization of PKM2 and absolves the Warburg effect induced in activated fibroblasts. By reducing Warburg effect, we have reduced the accumulation of glycolytic intermediates that serve as building blocks for the *de novo* synthesis of serine and glycine. Glycine is necessary for the assembly of collagen fibrils and treatment with PKM2 activators leads to glycine auxotrophy in these cells leading to dysregulated collagen fibrils and thereby reduced ECM secretion and deposition in the extracellular space of fibrotic organs. We tested our hypothesis in two different organ models of fibrosis, hepatic and pulmonary fibrosis. In both these models, the treatment with PKM2 activators reduced collagen synthesis and deposition. Treatment also reduced the morbidity and mortality in mice and improved their overall health and activity. We observed the reduced glycine levels in these organs post treatment and the reduced collagen load also lead to reduced inflammatory profile in these organs.

We further tested the effect of dimeric PKM2 and its association with HIF-1α in fibrotic organs. Hypoxia is known to be upregulated in these organs leading to the production of several HRE genes including LOX. LOX irreversibly crosslinks collagen and reduces collagen

degradation. Treatment with PKM2 activators reduced the association of PKM2 and HIF-1α and reduced its nuclear localization. This reduced the production of LOX and its family proteins and reduced crosslinking of collagen in the extracellular space thereby leading to its degradation by MMPs. We therefore concluded that the treatment with PKM2 activators leads to the alteration of the metabolic state of the activated fibroblasts and coupled with the reduced expression of HRE genes leads to the overall reduction in the fibrotic burden and increases overall survivability. Therefore, PKM2 activators are a novel category of therapeutic options for the treatment of fibrotic diseases.

5.8 Impact and Significance

The rise of fibrosis mediated liver and lung diseases in the USA has increased dramatically in the last few years. It has been noted that around 88,000 people die annually to alcohol related liver diseases. And around 40,000 people are diagnosed with idiopathic pulmonary fibrosis in the USA every year. The morbidity and mortality rates of these diagnosed individuals is high due to the lack of better treatment options to tackle fibrosis and its associated maladies. Here we show that using a metabolic approach, that the progress of fibrosis can be slowed by inducing the basal metabolic shift in activated myofibroblasts which are the main perpetrators of disease. This novel approach enables us to counter the fibrotic process and diminish disease progression. We believe that the activation of PKM2 using exogenous activators is a therapeutic option with high treatment potential to reduce the burden of fibrosis in these patients and decrease the morbidity and mortality and therefore increase longevity in patients suffering from fibrosis mediated liver and lung diseases.

REFERENCES

1. Berg, J. M., Tymoczko, J. L., Gatto, G. J., & Stryer, L. (2015). Biochemistry (Eighth edition. ed.). New York: W.H. Freeman & Company, a Macmillan Education Imprint.
2. Berg, R. A., & Prockop, D. J. (1973). The thermal transition of a non-hydroxylated form of collagen. Evidence for a role for hydroxyproline in stabilizing the triple-helix of collagen. Biochem Biophys Res Commun, 52(1), 115-120. doi:10.1016/0006-291x(73)90961-3
3. Canelon, S. P., & Wallace, J. M. (2016). beta-Aminopropionitrile-Induced Reduction in Enzymatic Crosslinking Causes In Vitro Changes in Collagen Morphology and Molecular Composition. PLoS One, 11(11), e0166392. doi:10.1371/journal.pone.0166392
4. Christofk, H. R., Vander Heiden, M. G., Harris, M. H., Ramanathan, A., Gerszten, R. E., Wei, R., . . . Cantley, L. C. (2008). The M2 splice isoform of pyruvate kinase is important for cancer metabolism and tumour growth. Nature, 452(7184), 230-233. doi:10.1038/nature06734
5. Christofk, H. R., Vander Heiden, M. G., Wu, N., Asara, J. M., & Cantley, L. C. (2008). Pyruvate kinase M2 is a phosphotyrosine-binding protein. Nature, 452(7184), 181-186. doi:10.1038/nature06667
6. Diegelmann, R. F., & Evans, M. C. (2004). Wound healing: an overview of acute, fibrotic and delayed healing. Front Biosci, 9, 283-289. doi:10.2741/1184

7. Gao, X., Wang, H., Yang, J. J., Liu, X., & Liu, Z. R. (2012). Pyruvate kinase M2 regulates gene transcription by acting as a protein kinase. Mol Cell, 45(5), 598-609. doi:10.1016/j.molcel.2012.01.001

8. Gorres, K. L., & Raines, R. T. (2010). Prolyl 4-hydroxylase. Crit Rev Biochem Mol Biol, 45(2), 106-124. doi:10.3109/10409231003627991

9. Gu, L., Zhu, Y. J., Yang, X., Guo, Z. J., Xu, W. B., & Tian, X. L. (2007). Effect of TGF-beta/Smad signaling pathway on lung myofibroblast differentiation. Acta Pharmacol Sin, 28(3), 382-391. doi:10.1111/j.1745-7254.2007.00468.x

10. Hata, A., & Chen, Y. G. (2016). TGF-beta Signaling from Receptors to Smads. Cold Spring Harb Perspect Biol, 8(9). doi:10.1101/cshperspect.a022061

11. Herchenhan, A., Uhlenbrock, F., Eliasson, P., Weis, M., Eyre, D., Kadler, K. E., . . . Kjaer, M. (2015). Lysyl Oxidase Activity Is Required for Ordered Collagen Fibrillogenesis by Tendon Cells. J Biol Chem, 290(26), 16440-16450. doi:10.1074/jbc.M115.641670

12. Hernandez-Gea, V., & Friedman, S. L. (2011). Pathogenesis of liver fibrosis. Annu Rev Pathol, 6, 425-456. doi:10.1146/annurev-pathol-011110-130246

13. Hosios, A. M., Fiske, B. P., Gui, D. Y., & Vander Heiden, M. G. (2015). Lack of Evidence for PKM2 Protein Kinase Activity. Mol Cell, 59(5), 850-857. doi:10.1016/j.molcel.2015.07.013

14. Hsu, M. C., & Hung, W. C. (2018). Pyruvate kinase M2 fuels multiple aspects of cancer cells: from cellular metabolism, transcriptional regulation to extracellular signaling. Mol Cancer, 17(1), 35. doi:10.1186/s12943-018-0791-3

15. Hsu, M. C., Hung, W. C., Yamaguchi, H., Lim, S. O., Liao, H. W., Tsai, C. H., & Hung, M. C. (2016). Extracellular PKM2 induces cancer proliferation by activating the EGFR signaling pathway. Am J Cancer Res, 6(3), 628-638. Retrieved from https://www.ncbi.nlm.nih.gov/pubmed/27152240

16. Huang, L., Yu, Z., Zhang, Z., Ma, W., Song, S., & Huang, G. (2016). Interaction with Pyruvate Kinase M2 Destabilizes Tristetraprolin by Proteasome Degradation and Regulates Cell Proliferation in Breast Cancer. Sci Rep, 6, 22449. doi:10.1038/srep22449

17. Israelsen, W. J., & Vander Heiden, M. G. (2015). Pyruvate kinase: Function, regulation and role in cancer. Semin Cell Dev Biol, 43, 43-51. doi:10.1016/j.semcdb.2015.08.004

18. Jiang, Y., Wang, Y., Wang, T., Hawke, D. H., Zheng, Y., Li, X., . . . Lu, Z. (2014). PKM2 phosphorylates MLC2 and regulates cytokinesis of tumour cells. Nat Commun, 5, 5566. doi:10.1038/ncomms6566

19. Li, L., Zhang, Y., Qiao, J., Yang, J. J., & Liu, Z. R. (2014). Pyruvate kinase M2 in blood circulation facilitates tumor growth by promoting angiogenesis. J Biol Chem, 289(37), 25812-25821. doi:10.1074/jbc.M114.576934

20. Mukherjee, J., Ohba, S., See, W. L., Phillips, J. J., Molinaro, A. M., & Pieper, R. O. (2016). PKM2 uses control of HuR localization to regulate p27 and cell cycle progression in human glioblastoma cells. Int J Cancer, 139(1), 99-111. doi:10.1002/ijc.30041

21. Ricard-Blum, S. (2011). The collagen family. Cold Spring Harb Perspect Biol, 3(1), a004978. doi:10.1101/cshperspect.a004978

22. Ryan, D. G., Murphy, M. P., Frezza, C., Prag, H. A., Chouchani, E. T., O'Neill, L. A., & Mills, E. L. (2019). Coupling Krebs cycle metabolites to signalling in immunity and cancer. Nat Metab, 1, 16-33. doi:10.1038/s42255-018-0014-7

23. Sauk, J. J., Nikitakis, N., & Siavash, H. (2005). Hsp47 a novel collagen binding serpin chaperone, autoantigen and therapeutic target. Front Biosci, 10, 107-118. doi:10.2741/1513

24. Shoulders, M. D., & Raines, R. T. (2009). Collagen structure and stability. Annu Rev Biochem, 78, 929-958. doi:10.1146/annurev.biochem.77.032207.120833

25. Smith-Mungo, L. I., & Kagan, H. M. (1998). Lysyl oxidase: properties, regulation and multiple functions in biology. Matrix Biol, 16(7), 387-398. doi:10.1016/s0945-053x(98)90012-9

26. Vander Heiden, M. G., et al. (2009). "Understanding the Warburg effect: the metabolic requirements of cell proliferation." Science 324(5930): 1029-1033.

27. Vander Heiden, M. G., Christofk, H. R., Schuman, E., Subtelny, A. O., Sharfi, H., Harlow, E. E., . . . Cantley, L. C. (2010). Identification of small molecule inhibitors of pyruvate kinase M2. Biochem Pharmacol, 79(8), 1118-1124. doi:10.1016/j.bcp.2009.12.003

28. Wuyts, W. A., Agostini, C., Antoniou, K. M., Bouros, D., Chambers, R. C., Cottin, V., . . . Verleden, G. M. (2013). The pathogenesis of pulmonary fibrosis: a moving target. Eur Respir J, 41(5), 1207-1218. doi:10.1183/09031936.00073012

29. Wynn, T. A. (2008). Cellular and molecular mechanisms of fibrosis. J Pathol, 214(2), 199-210. doi:10.1002/path.2277

30. Yang, W., Xia, Y., Ji, H., Zheng, Y., Liang, J., Huang, W., . . . Lu, Z. (2011). Nuclear PKM2 regulates beta-catenin transactivation upon EGFR activation. Nature, 480(7375), 118-122. doi:10.1038/nature10598

31. Zhang, Y., Li, L., Liu, Y., & Liu, Z. R. (2016). PKM2 released by neutrophils at wound site facilitates early wound healing by promoting angiogenesis. Wound Repair Regen, 24(2), 328-336. doi:10.1111/wrr.12411